KINETICS OF NONHOMOGENEOUS PROCESSES

A PRACTICAL INTRODUCTION FOR CHEMISTS, BIOLOGISTS, PHYSICISTS, AND MATERIALS SCIENTISTS

Edited by
Gordon R. Freeman
University of Alberta

CONTENTS

7 MODELS OF CELLULAR RADIATION ACTION

Albrecht M. Kellerer

Institut für Medizinische Strahlenkunde
der Universität Würzburg
Würzburg, Federal Republic of Germany

7.1. INTRODUCTION

Living cells can be affected by exposure to chemicals or to ionizing radiation. The resulting effects are not inherently different. However, it is a singular feature of ionizing radiation that energy is transmitted to the exposed media in discrete packages and that the microdistribution of imparted energy and of subsequent radiation products is highly nonuniform. This nonuniformity determines the relative biological effectiveness of different types of ionizing radiation, and its role is particularly important at small doses. Nonhomogeneous kinetics is, therefore, a central issue in radiation biophysics.

The physics of the interaction of ionizing radiation with matter and the spatial distributions of energy in charged particle tracks are treated in detail in Chapter 3. Figure 7.1 is a simplified diagram of tracks of sparsely and densely ionizing charged particles in relation to the superimposed micrograph of part of a mammalian cell. The microdistribution of energy has always been a principal topic of quantitative radiobiology. It is also the subject of microdosimetry, a new branch of dosimetry and radiation physics created by H. H. Rossi. Despite the more rigorous concepts of microdosimety, semiquantitative treatments—for example, in terms of the concept of linear energy transfer (LET)—are still common. To put the different approaches into perspective, it is necessary to deal first with simple approaches and with the theories of radiation action that preceded microdosimetry. Most of the models treated in Section 7.2 are too crude to be of pragmatic value in themselves. The basic probabilistic notions are, however, essential, and to understand the simplified approaches and their limitations is a condition for the development and utilization of more sophisticated treatments.
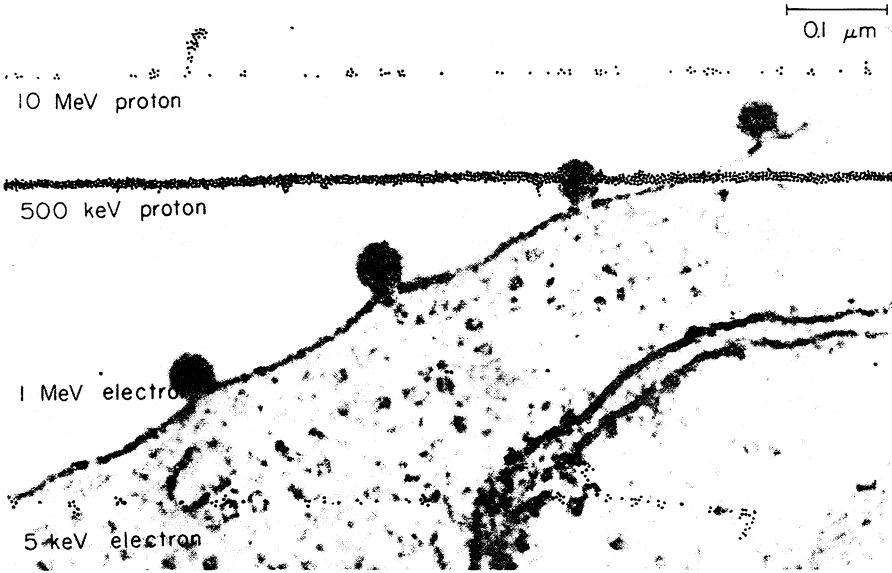
Figure 7.1. Diagram of charged particle tracks superimposed on a micrograph (adapted from Ref. 1) of part of a mammalian cell. The viruses budding from the outer cell membrane permit an added comparison of size. In the projected track segments the dots represent ionizations. The lateral extension of the track core is somewhat enlarged in order to resolve the individual energy transfers. For more accurate diagrams of particle tracks see Chapter 3.

7.2. ESSENTIALS OF TARGET THEORY

Quantitative radiobiology began with investigations of the inactivation of bacteria, viruses, or certain enzymes by X rays. In such experiments dose–effect relations were found that differ characteristically from those familiar in cytotoxicology. The differences are fundamental to an understanding of the action of ionizing radiations. An initial, general consideration of dose–effect relations is, therefore, required.

The simplest dose dependence would result if the exposed organism, for example, a bacterium, tolerated doses up to a certain threshold but were inactivated if this threshold were exceeded. The dose–effect relation would then be a step function. In reality, one can never attain entirely homogeneous populations in microbiological studies. Furthermore, one must note that biological processes are inherently stochastic; the complexity even of simple cells is such that the slightest differences in initial conditions can lead to unpredictable fluctuations in the response to various factors. Although such systems are in principle deterministic,
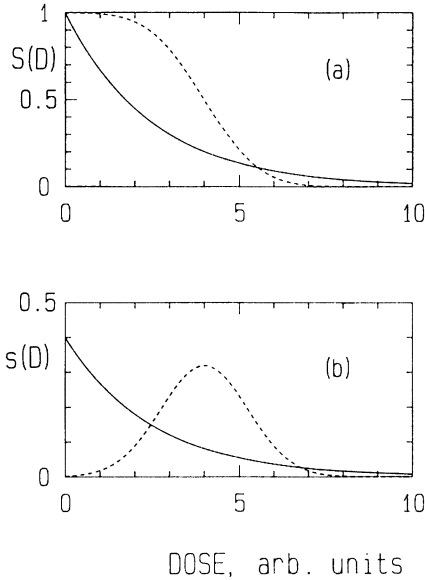
Figure 7.2. Exponential and sigmoid dose-effect relations and their derivatives.

their reactions can be described only in stochastic terms. Instead of the threshold reaction, one expects a response curve such as the dashed line in Figure 7.2. Dependences of this type are termed *sigmoid curves* or *shoulder curves*.

A naive explanation of a sigmoid dose–effect relation invokes the notion of a distribution of sensitivities within a population. The stochastic response of the cell is not considered. Instead it is assumed that individuals of the population have different critical thresholds of dose. If, for example, one postulates the Gaussian distribution of critical doses symbolized in Figure 7.2*b*, one obtains the integral of this distribution, that is, the sigmoid curve in Figure 7.2*a*, as a response function. The example shows that the derivative, $-dS(D)/dD$, of the survival curve can, in the simplest interpretation, be considered as the probability distribution of critical doses; one could also speak of the probability distribution of resistance within the population. However, this interpretation in terms of biological variability is only one among other possibilities. It disregards the potential influence of other stochastic factors that may codetermine the dose–response relation.

In early radiobiological experiments, when enzymes, viruses, or certain bacteria were exposed to X rays, entirely different dose–effect relations were obtained (2). The fraction of viable units, $S(D)$, decreases—as exemplified in Figure 7.3 for the DNA phage T7—exponentially with the absorbed dose D:*

$$S(D) = \exp(-aD) \qquad (7.1)$$

*The form of Eq. (7.1) is similar to that of Eq. (6.56), where the parameter N, is analogous to D and nf_{tr} is analogous to a. Both equations are based in stochastics. (Ed.)
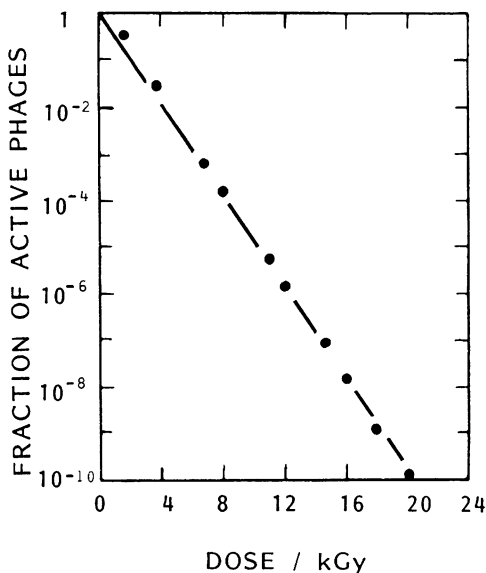
Figure 7.3. Exponential dose dependence for the inactivation of T1 phages by Co γ rays (redrawn from Ref. 3).

The solid line in Figure 7.2a corresponds to this relation. The distribution of resistance that could explain such a curve would also be an exponential, as shown in Figure 7.2b (solid line):

$$\frac{-dS(D)}{dD} = s(D) = a \exp (-aD) \tag{7.2}$$

This distribution has its maximum at $D = 0$, that is, a relatively large fraction of the exposed entities would have to be highly sensitive. The broad tail would imply, on the other hand, that a substantial fraction of the microbiological entities is highly resistant. Biological variability cannot, in general, be the reason for such relations. However, analogy to radioactive decay led to a different interpretation that was to become the basis of target theory (2, 4–6).

7.2.1. Exponential Dose–Effect Relation and Single-Hit Process

The decay of a radioactive substance is characterized by the fact that equal fractions of the remaining atoms disintegrate in equal time intervals:

$$\frac{dN(t)}{N(t)} = -a \, dt \quad \text{or} \quad \frac{d \ln N(t)}{dt} = -a \tag{7.3}$$

Therefore,

$$N(t) = N_0 \exp(-at) \tag{7.4}$$

where $N(t)$ is the number of atoms still present at time t. The probability of an atom to disintegrate is, accordingly, independent of its age. This independence reflects the fact that the decay process is a spontaneous random event rather than the result of gradual deterioration.

The interpretation of the exponential survival curves in radiobiology is analogous. Dose takes the place of time; with constant dose rate it is proportional to time. Regardless of the dose already applied, a constant dose increment reduces the number, $N(D)$, of survivors by a constant fraction:

$$\frac{dN(D)}{N(D)} = -a\, dD \quad \text{or} \quad \frac{d\ln N(D)}{dD} = -a \tag{7.5}$$

Therefore,

$$N(D) = N_0 \exp(-aD) \tag{7.6}$$

Normalized to the surviving fraction, $S(D) = N(D)/N_0$, one has

$$S(D) = \exp(-aD) \tag{7.7}$$

The exponential survival curves can, therefore, be understood in terms of individual random events. Such random events have been called hits because they had to be discrete acts of energy transfer from the radiation field to sensitive structures of the exposed organism. Dessauer introduced the notion of *point heat* to characterize the hit process (7). Crowther, who developed the formalism of target theory independently (8), postulated somewhat more pragmatically that the hits were individual ionizations in the sensitive structures. His assumption has been verified in many radiobiological investigations on enzymes. or single-strand viruses. It was demonstrated that such comparatively simple systems can, indeed, be inactivated by the detachment of individual electrons, with subsequent damage caused directly, or induced indirectly, through the formation and action of free radicals.

From Eq. (7.5) one concludes that $a\, dD$ is the probability of a hit per dose increment, dD. Accordingly, aD is the mean number of hits per exposed unit at dose D. Assuming a certain magnitude E of energy deposition in individual events (ionization or cluster of ionizations), one can utilize this relation to deduce formally a *critical mass* or a corresponding *critical volume*. The example of Figure 7.3 may explain the method. The T1 phage is inactivated according to Eq. (7.7) with $a = 0.0011\ \mathrm{Gy}^{-1}$. The mean number of hits in the assumed target region is then aD, and the mean energy per target region is aDE. The mean energy is also equal to the dose times the mass m of the target region:

$$aDE = Dm \qquad (7.8)$$

Therefore,

$$m = Ea \qquad (7.9)$$

For example, if one primary ionization corresponds to the mean energy transfer E = 80 eV, one has (with 1 eV = 1.602×10^{-19} J and 1 Gy = 1 J/kg):

$$m = Ea = 80 \text{ eV} \times 0.0011 \text{ } Gy^{-1} = 80 \times 1.6 \times 10^{-19} \times 0.0011 \text{ kg}$$
$$= 1.4 \times 10^{-17} \text{ g} \qquad (7.10)$$

The actual mass of the DNA double-strand molecule of the T1 phage is 5×10^{-17} g. The inactivation probability due to a single collision is thus substantially less than 1. It is likely that the critical events are those that produce a double-strand break in the phage DNA.

7.2.1.1. Geometric Illustration of Single-Hit Process.

The single-hit mechanism is a comparatively simple random process. Other schemes are considered in subsequent sections of this chapter. To elucidate the relations between the processes of different complexity, simplified two-dimensional schemes are employed. Such schemes can also be used to illustrate the single-hit process and to bring out certain factual deviations from the model.

The three panels in Figure 7.4 illustrate schematically the occurrence of absorption events (hits) in individual cells, which are represented as squares and rectangles. The dots symbolize energy deposits (ionizations) randomly occurring within the collective of cells.

Panel A depicts the simplest case where all cells are of equal sizes and consequently have equal probabilities to be hit. Panel B gives cells of varying sizes,
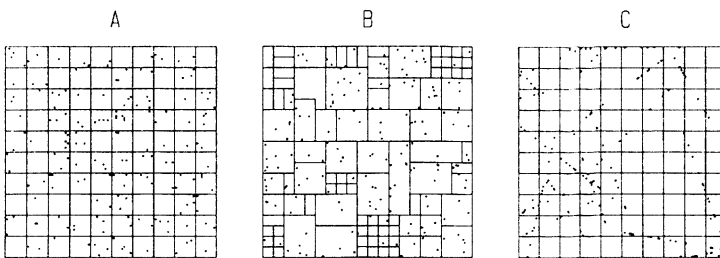
Figure 7.4. Diagrams of different Poisson processes with an average number of 1.8 hits/cell. Panel A: Simple Poisson process of independent hits on cells of equal size. Panel B: Simple Poisson process of independent hits on cells of varying size. Panel C: Poisson process of spatially correlated hit events, also termed compound Poisson process.

with corresponding variation of the probabilities to be hit. Panel C represents, again, an array of equal cells. However, the energy deposits occur in clusters, which are simplified two-dimensional analogs of charged particle tracks.

The panels give the random configurations at a specified "dose". Dose is here measured in terms of the mean number of events per exposed unit, the value being 1.8 in the example of Figure 7.4. The graphs of Figure 7.5 represent results of simulated exposures. The decreasing number of undamaged cells (that is, cells still without a hit) is plotted versus dose. The somewhat irregular functions result from the relatively small size of the samples of only 100 cells. If the number of cells were vastly increased, or if many repeated simulations were performed, one would obtain the dashed lines in the graphs.

The simplest case of equal cells in panel A (that is, the case with no biological variability) results in an exponential survival curve. One speaks of a pure Poisson process.

The more complex case of panel B (that is, the case that corresponds to cells with different sensitivities) results in a curve that is not straight in the semilogarithmic plot but is concave upward. This is understood from the fact that the smaller units, which represent the more resistant cells, tend to survive to higher doses, so that the average sensitivity (that is, the probability to be hit) of the survivors declines with increasing dose. Accordingly, the slope of the survival curve in the semilogarithmic plot decreases at higher doses.

Panel C represents the case of spatial correlation of some of the energy deposits. Such spatial correlation—the central aspect of microdosimetry—occurs in charged particle tracks; it has the general effect that there are fewer energy deposition events
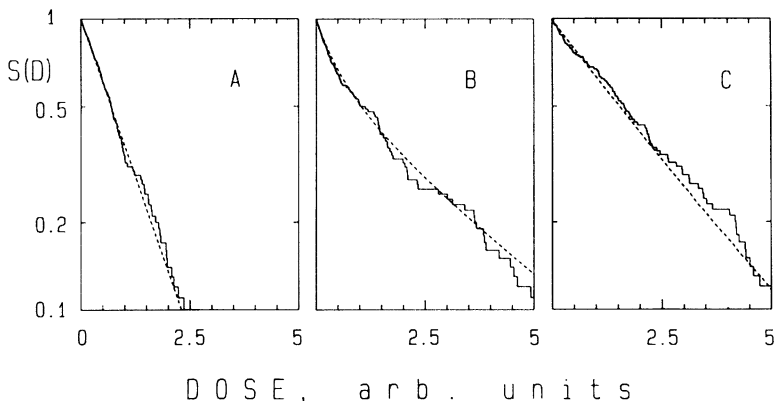
Figure 7.5. The elimination of cells with increasing dose in the samples of Figure 7.4. The step functions are the results of random trials; the broken curves apply to large samples. For the assumed one-hit process the dependences are exponential if the cells are of equal size (case A and C). The spatial correlation of hits (case C) reduces the slope of the dose dependence. The differences in sensitivity (case B) cause a nonexponential dependence.

(passages of charged particles) per cell but there can be multiple ionizations per event. Due to the statistical independence of events, one obtains an exponential dose dependence, but the reduced event frequency causes a reduced slope of the survival curve; in other words, the close spatial correlation of energy transfers creates some waste of energy in the single-hit process. A radiation of higher ionization density has in general less biological effectiveness. In a multihit process, that is, in a case where damage accumulation is required for the biological effect, the situation can be reversed (Section 7.2.2).

7.2.2. Interpretation of Sigmoid Dose–Effect Relations

When target theory was conceived for the interpretation and quantitative analysis of single-hit processes, it opened up an intriguing new field of study to the biophysicist. The term *quantum biology* was coined (4). It referred to the fact that the detachment of single electrons could have substantial effects on complex cellular systems containing billions of atoms. It was natural, in view of the fascination with a novel field of research, that attempts were made to explore also broader implications beyond the immediate scientific issues, and such considerations extended to general philosophical discussions of determinism or indeterminism in living objects (9). The formalism of target theory was also extended, and attempts were made to explain all survival curves—not merely the exponential ones—in terms of the statistics of energy deposition.

Sigmoid dose dependences are obtained when certain bacteria or, as in the example of Figure 7.6, higher cells are exposed to X or γ rays. The assumption was made that with these dose relations also, the deviations from a step function are caused by the statistics of energy deposition. Later it was recognized that this must be an oversimplification, and the deviations are the composite result of several factors, among which the fluctuations of energy deposition need not always be the dominant one. It is nevertheless useful to review the classical multihit or multitarget models, even if they have little pragmatic importance. The underlying mathematics is, in modified form, required in any treatment of the statistics of energy deposition by ionizing radiations. The subsequent considerations serve as a simple introduction to necessary elements of probability theory. In particular, the Poisson distribution and the closely related Γ distribution will be referred to.

7.2.2.1. Multihit Process and Poisson Distribution. The slope of the survival curve in the semilogarithmic representation, $-d(\ln S(D))/dD$, is constant for the exponential relation. For sigmoid curves it increases with increasing dose, and this is the expression of a gradual accumulation of damage. The slope determines the fraction of the surviving cells that is inactivated by an additional dose increment. The slope increases with absorbed dose in those cases where successive hit events accumulate damage up to a critical level.

The simplest model of a multihit process results from the assumption of a definite threshold, that is, from the postulate that the cell survives with less than n
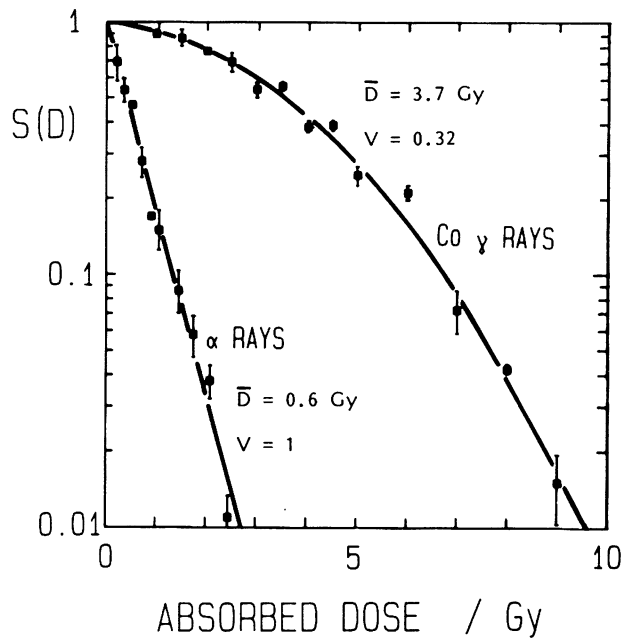
Figure 7.6. Loss of proliferative ability of mouse fibroblast cells exposed to Co γ rays and americium α rays. Data are from experiments by Lücke-Huhle et al. (10). Parameters: mean inactivation dose $\bar{D}$ and relative variance V are indicated for the two survival functions; for definitions see Section 7.2.4.

hits but is inactivated if there are n or more hits. If the hits are statistically independent, and if all exposed units have the same critical threshold n, one obtains comparatively simple equations.

The Poisson equation gives the probability for exactly ν events in a trial, when the number of events averaged over many trials is x:

$$p(\nu) = \exp(-x)\frac{x^{\nu}}{\nu!} \tag{7.11}$$

This relation can be illustrated in terms of panel A in Figure 7.4. The average number of events per field in the diagram is $N = 1.8$. Figure 7.7 gives for this expectation value the Poisson distribution and a corresponding sum distribution:

$$P(\nu) = \sum_{k=0}^{\nu-1} \exp(-x)\frac{x^{k}}{k!} \tag{7.12}$$

Inserted in Figure 7.7 as dashed lines are also the graphs that correspond to the particular trial represented in panel A of Fig. 7.4 for the sample of 100 cells.

For the Poisson distribution the variance σ^2 is equal to the mean x, and the

NUMBER OF HITS, ν
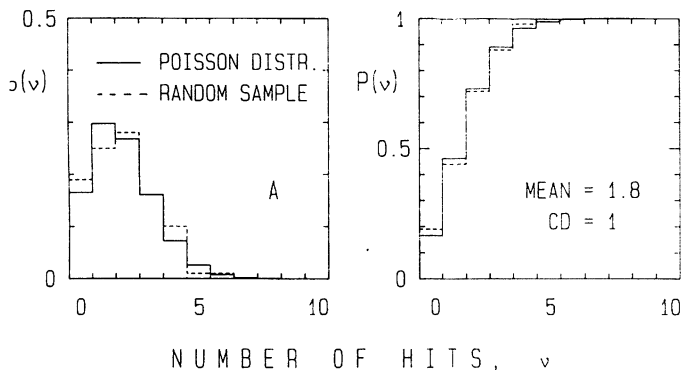
Figure 7.7. Poisson distribution of hits for the expectation value 1.8 and its sum distribution (solid lines). Broken lines are frequencies resulting from a random trial with the sample of 100 cells in panel A of Figure 7.4. The value 1 of the coefficient of dispersion (CD) applies to Poisson distributions regardless of their mean value.

dispersion coefficient, $CD = \sigma^2/x$, is equal to unity. The dispersion coefficient for the data from panel A (Figure 7.4) is

$$CD = \sum_{i=1}^{I} \frac{(\nu_i - x)^2}{Ix} = 0.99 \approx 1 \qquad (7.13)$$

where ν_i is the number of events in cell i ($i = 1, \ldots, I$), and $x = 1.8$ the mean number of events per cell, which is estimated as $x = \Sigma \nu_i/I$.

Figure 7.8 gives, for comparison, the distribution of the number of hits per cell
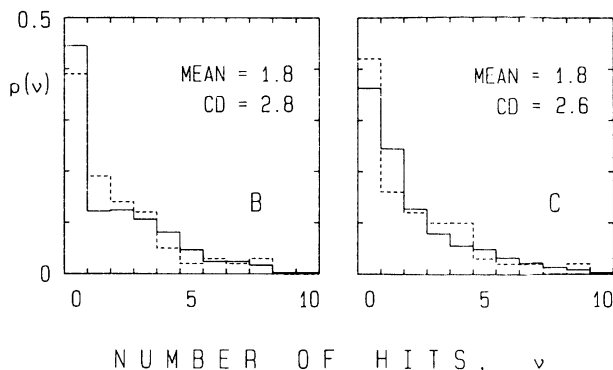
NUMBER OF HITS, ν

Figure 7.8. Relative frequencies of the number of hits at a mean value of 1.8 hits/cell for the processes B and C in Figure 7.4. Broken lines are the results of random trials for the samples of 100 cells. The solid lines and the coefficients of dispersion apply to large samples.

for the two random trials in panels B and C of Figure 7.4. The distributions are substantially broader, and the coefficients of dispersion are 2.8 and 2.6. Biological variability of sensitivity enhances, in the same way as the statistics of energy deposition, the fluctuations of the effect on individual cells.

According to the multihit model, all those cells survive that have less than n hits. With $x = aD$, the survival function is

$$S(D) = \sum_{\nu=0}^{n-1} \exp(-aD) \frac{(aD)^\nu}{\nu!} \tag{7.14}$$

Figure 7.9 represents the multihit relations (i.e., the survival functions according to this equation) for selected values of the parameter n. As expected, the shoulder of the curves is most pronounced for large n; the stochastic character of the response is less marked when many random events must be accumulated to reach the critical level of damage.

The steplike function in Figure 7.9 gives the result of the random simulation of a three-hit process corresponding to the simple Poisson process represented in panel A of Figure 7.4. Although the result is obtained with the comparatively small sample of only 100 cells, it is in general accord with the theoretical curve for $n = 3$.

The more complex conditions represented in Figure 7.4 can be utilized to illustrate fundamental inadequacies of the simple multihit model. Figure 7.10 com-
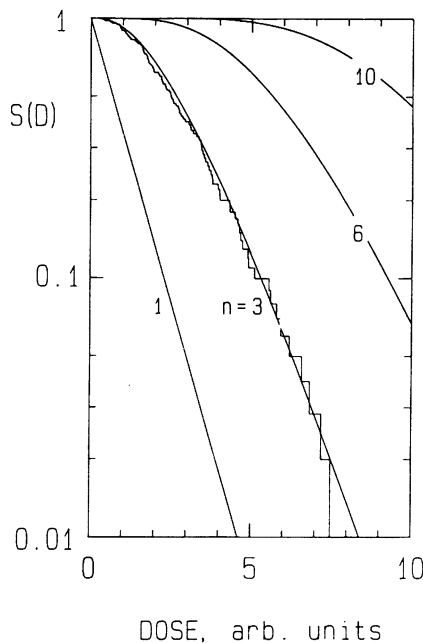
Figure 7.9. Multihit survival curves according to Eq. (7.14). Values aD are given on the abscissa. The random curve results from a trial of a three-hit process on the sample of 100 equal cells in panel A of Figure 7.4.
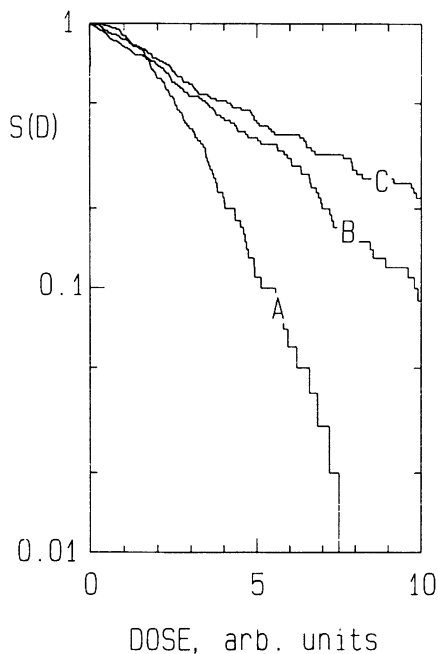
Figure 7.10. Comparison of three-hit survival curves obtained from random trials of the processes A, B, and C in Figure 7.4. Deviations from the simple Poisson process (A), such as varying size of the cells (B) or spatial correlation of hits (C), lead to a reduction of the shoulder, that is, to an increased relative variance of the survival functions (see Section 7.2.4).

pares the survival relations obtained from random trials for the samples of 100 cells for the three cases and an assumed three-hit process. The result for case *B* illustrates the general effect that any variations of sensitivity decrease the shoulder of the curve. This fact has frequently been overlooked in applications of multihit theories to observed survival curves where it was usually assumed that the combined influence of all factors other than the statistics of energy deposition would somehow "average out." Instead, the general effect is one of reducing the apparent hit numbers. Such numbers may, therefore, be misleading and quite meaningless as estimates of the multiplicity of events involved in the cellular action of ionizing radiations.

Curve *C* illustrates the influence of the spatial correlation of energy deposits within charged particle tracks. Spatial correlation of energy deposits, too, leads to a reduction of the shoulder of the survival curve, that is, to smaller apparent hit numbers. This is in agreement with the general observation that survival functions, as well as other dose–effect relations, for sparsely ionizing radiations can have pronounced shoulders while relations obtained with densely ionizing radiations tend to be exponential (see Figure 7.6). The explanation is that if more energy is imparted to the cell in one event, fewer events are required on the average to reach the critical level of damage. In Section 7.2.4 the relative variance V of the dose–effect relation is defined, a parameter that quantifies the extent of the deviations from a threshold response. For the survival curves of Figure 7.6 one obtains the value $V = 0.32$ for γ rays and $V = 1$ for α rays.

7.2.2.2. Time Factor. The simple multihit model postulates accumulation of damage due to random events that are statistically independent. The model disregards the additional factors that codetermine the response of the irradiated cells. One factor, beyond those that have been considered, is the temporal distribution of dose. DNA is the major target of radiation damage in the cell, and there are various repair mechanisms that eliminate or reduce damage to DNA. The time constants of the repair processes are seconds to hours. Due to the repair processes, a short-term irradiation is, in general, more effective than the protracted or fractionated application of the same dose. When there is sufficient time during the irradiation for partial reversion of sublethal damage, the accumulation of damage and the subsequent radiation effects are reduced.

Because of the oversimplified nature of the multihit model, there is little justification for formal modifications of the equations that would account for the dose-rate effect. But even without a quantitative treatment, it is helpful to illustrate the general influence of the time factor. One can postulate that the sublesions produced by individual hits are restituted randomly with constant probability *b* per unit time. There is then an exponential distribution of lifetimes of the lesions. It is easy to simulate such a model. The results in Figure 7.11A are two-hit curves for the simple Poisson process (i.e., the random process represented in panel A of Figure 7.4); they are derived with the assumed repair process under the condition of constant dose rate, which is most common in practice. Random trials for the sample
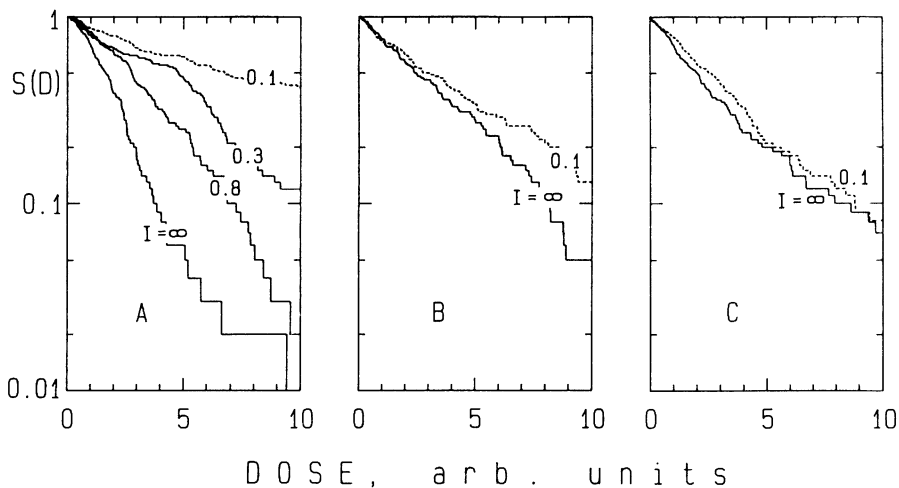
Figure 7.11. Influence of dose rate on two-hit curves resulting from random trials for the processes in panels A, B, and C in Figure 7.4. Parameter *I* corresponds to the dose rate; it equals the mean number of hits per cell during the mean restitution time. The influence is largest for the pure Poisson process (A). It is substantially reduced for the process with different cell sizes (B), and it is nearly absent in the process with spatially correlated hits (C).

of 100 cells are given for different dose rates. The dose rate I is here expressed as the ratio of the mean number of hit events per unit time and the repair rate b:

$$I = \frac{a\ (dD/dt)}{b} \tag{7.15}$$

The general result is that the survival curves have substantially reduced shoulders when the dose rate is sufficiently small for the influence of repair to become important. This is in agreement with a wide range of experimental results.

According to the simple model, the probability of an observable effect can be vanishingly small at very small dose rates. In most experimental systems such a complete reduction is not observed, and there are two main reasons. The first is that part of the cellular damage can be irreversible. The second reason is that the statistical fluctuations of energy deposition are such that even with sparsely ionizing radiations single charged particles can, with small probability, bring about effects that usually require the accumulation of several energy deposition events. Figure 7.11C shows that, in fact, the dose–rate dependence is substantially reduced for a model that includes spatial correlations of energy transfers (panel C of Figure 7.4). For densely ionizing radiations this microdosimetric aspect, the instantaneous local energy accumulation, is the predominant characteristic. Dose–rate dependences of cellular effects are then largely absent. On the tissue level dose–rate effects can occur even with densely ionizing radiations, but they do not always consist in a reduction of the effect with protraction or fractionation of an exposure (11).

7.2.3. Limited Validity of Target Theory Models

As pointed out in the preceding sections, the multihit theory is a gross oversimplification because it attempts to explain the dose–effect relation merely in terms of the statistics of energy deposition, disregarding other factors that codetermine the dose dependences. It is, nevertheless, possible to derive from observed dose–effect relations certain rigorous statements on the accumulation of damage in independent events of energy deposition. This is considered in Section 7.2.4.

7.2.3.1. A More General Treatment in Terms of Markov Processes. The multihit model is the simplest description of a process of random accumulations of damage. The same mathematical relations have been postulated in multistep theories of cancer. There are, nevertheless, a variety of alternative models.

One familiar model is the multitarget postulate. It is assumed that there are m targets in the cell and that all targets have to be damaged if the effect is to occur. Making the simplest assumption of independent single-hit inactivation of the individual targets with equal probabilities, one obtains the survival function

$$S(D) = 1 - [1 - \exp{(-aD)}]^m \tag{7.16}$$

This equation can describe adequately the inactivation of clumps of m cells if the survival relation of the individual cell is exponential. But apart from this nearly trivial example, there have never been experiments where a response function has been fitted by the equation and where such a fit has then led to the identification of the corresponding number of actual critical structures.

With a modification to account for the finite initial slope of dose–effect relations at small doses and with the admission of noninteger values for the exponent m, the equation

$$S(D) = \exp\left(-cD\right)\left\{1 - \left[1 - \exp\left(-aD\right)\right]^m\right\} \qquad (7.17)$$

is frequently used to describe observed survival functions, for example, of mammalian cells, exposed to sparsely ionizing radiations. However, it is realized that the applicability of the equation provides no verification of the underlying model; the fit is merely empirical.

The multitarget equation differs from the multihit equation chiefly by the fact that the curves have asymptotic tangents in the semilogarithmic representation. For both Eqs. (7.16) and (7.17) these tangents intersect the ordinate at the value m. One speaks of an "extrapolation number" rather than a "target number" in order to avoid the identification of the equation with the underlying target theory model.

A vast variety of other models could be postulated, but it makes little sense to employ equations that contain sufficient free parameters to fit nearly any dose-response relation. To put the target theory models into a more general context, it is nevertheless helpful to consider a broader class of stochastic models that contains the multihit or multitarget conditions as special cases. These are linear stochastic processes, which can be depicted as Markov chains (multicompartment models). Figure 7.12 gives diagrams that represent the multihit process, the multitarget process, and an example of a somewhat more general two-hit process. The latter model includes repair and also a single-hit component that may correspond to the action of densely ionizing radiation. In the diagrams the dots represent successive states of damage. The lowest dot represents the undamaged state, and the highest dot represents cell death or another specified irreversible effect. The coefficients of transition into states of higher damage are proportional to the dose rate I if time is chosen as the independent variable. The coefficients for the restitution processes are taken to be constant in the simple treatment referred to in the preceding paragraph. However, it is evident that there could be further complexities, such as a dependence of the repair rates on dose or on dose rate.

The purpose of the present discussion is not a detailed formal treatment but the critical assessment of somewhat arbitrary assumptions underlying all simplified models. More complex linear models could be constructed, and nonlinearities would lead to further complexities.

The linear models can always be represented by the simple equation
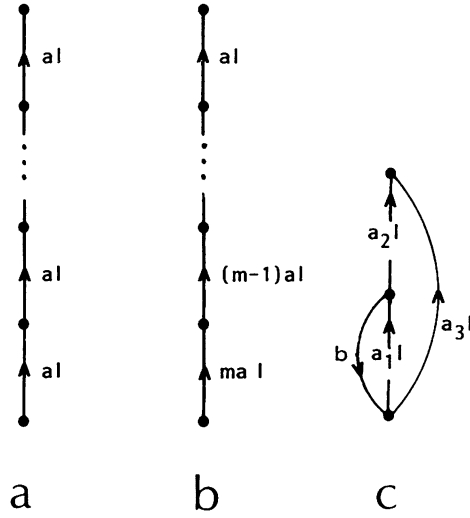
Figure 7.12. Schematic diagram of Markov processes that correspond to the multihit model [Eq. (7.14)], the multitarget model [Eq. (7.16)], and a two-hit process with repair [Eq. (7.19)].

$$\frac{d}{dD} X = AX \tag{7.18}$$

where X is a column vector that contains as components the probabilities for the individual states, say $0, \ldots, n - 1$; the last state need not appear in the equation, since its probability is the complement of the sum of all other probabilities. The matrix A contains the transition probabilities. The solution $X(D)$ can be given in terms of the eigenvectors and eigenvalues of the transition matrix A (6, 12).

The matrix of transition coefficients characterizes a particular model, and the solution for any such model is then straightforward. For example, Eqs. (7.14) and (7.16) are derived from Eq. (7.18) with the transition matrices that correspond to Figs. 7.12a, b. The transition matrix for Fig. 7.12c but with dose as independent variable is

$$A = \begin{pmatrix} -a_1 - a_3 & \dfrac{b}{I} \\ a_1 & -a_2 - \dfrac{b}{I} \end{pmatrix} \tag{7.19}$$

For the dose dependence of the survival $S(D)$, that is, the sum of the probabilities of the two states 0 and 1, one obtains

$$S(D) = c \exp(-\lambda_1 D) + (1 - c)\exp(-\lambda_2 D) \qquad (7.20)$$

with the eigenvalues:

$$\lambda_{1,2} = \frac{1}{2}\left(a_1 + a_2 + a_3 + \frac{b}{I} \pm \sqrt{\left(-a_1 + a_2 - a_3 + \frac{b}{I}\right)^2 + \frac{4a_1 b}{I}}\right)$$

and

$$c = \frac{\lambda_2 - a_3}{\lambda_2 - \lambda_1}$$

Somewhat different expressions result if the two eigenvalues are equal.

The comparatively simple two-event process has special interest because, as pointed out in later sections, cellular effects of ionizing radiations appear to result largely from second-order processes.

7.2.4. Generalized Characterization of Dose–Effect Relations

It has been shown in the preceding sections that the shoulder of a dose–response curve can be reduced by a variety of factors. The statistics of energy deposition is one of these, but this need not always be the dominant influence. To quantify statements on the shape of the dose–effect relation, one can utilize basic parameters that apply if the dose–response relation is treated formally as a probability distribution function. This notion was invoked at the beginning of this chapter in a specific explanation of a dose–effect relation as the sum distribution of the resistance of microorganisms (Section 7.2, Figure 7.2). As a general way to look upon dose–effect relations, the concept is, however, not sufficiently familiar, and it is helpful to illustrate it first in terms of the elementary Poisson process postulated by the multihit model.

Figure 7.13 represents several random paths that correspond to the Poisson process of equal independent events occurring with constant probability per unit dose. The vertical dotted line indicates a specified dose. The random lines intersect this line at integer ordinate values equal to the number of hits that have occurred. The distribution of the points of intersection follows the Poisson distribution. With a slight change in notation, Eq. (7.11) for the Poisson density (that is, the probability for exactly n events) is written as

$$p(n;x) = \exp(-x)\frac{x^n}{n!} \qquad (7.21)$$

EXPECTED NUMBER OF HITS
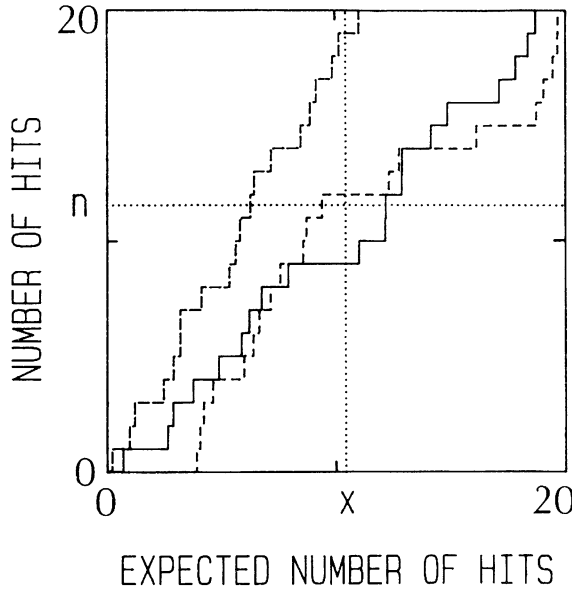
Figure 7.13. Three random paths for the simple Poisson process. The points of intersection with the vertical dotted line are subject to a Poisson distribution [Eq. (7.20)] with mean value $x = 10.4$. The points of intersection with the horizontal dotted line are subject to a gamma distribution [Eq. (7.23)] of order $n = 12$.

Equation (7.12) for the sum distribution takes the form

$$P(n; x) = \sum_{\nu=0}^{n-1} \exp(-x) \frac{x^\nu}{\nu!} = 1 - \int_0^x \exp(-z) \frac{z^{n-1}}{(n-1)!} dz \qquad (7.22)$$

where the last equality is obtained by taking the derivative with respect to x of the sum.

In its interpretation as the Poisson sum distribution $P(n; x)$ is the probability that a random path traverses the vertical line below n. An equivalent condition is that the random path intersects the horizontal dotted line at a value in excess of x. Therefore, $G(x; n) = 1 - P(n; x)$ is the sum distribution of values x to reach n events. The corresponding density is designated by $g(x; n)$; this is the differential distribution of the values x required to reach n events:

$$G(x; n) = \int \exp(-z) \frac{z^{n-1}}{(n-1)!} dz \qquad (7.23)$$

$$g(x; n) = \exp(-x) \frac{x^{n-1}}{(n-1)!} \qquad (7.24)$$

The distribution function $G(x; n)$ and the density of the random variable x are called Γ distributions of order n. For different values of the parameter n, the distributions are depicted in Figure 7.14.

The connection between the sum distributions $P(n; x)$ and $G(x; n)$ remains valid for a more general process with steps of variable size that correspond to the highly variable energy deposition by charged particles (see Section 7.4). The expressions for the densities relative to n or x are, however, different in this case. The subsequent relations for the moments are also specific to the pure Poisson process.

The mean value of the Γ distribution and its second moment are

$$\bar{x} = \int_0^\infty x \exp(-x) \frac{x^{n-1}}{(n-1)!} dx = n \tag{7.25}$$

$$\overline{x^2} = \int_0^\infty x^2 \exp(-x) \frac{x^{n-1}}{(n-1)!} dx = n(n+1) \tag{7.26}$$

As with the Poisson distribution the variance is equal to the mean:

$$\sigma^2 = \overline{x^2} - \bar{x}^2 = n \tag{7.27}$$

and the relative variance V is the inverse of the mean:

$$V = \frac{\sigma^2}{\bar{x}^2} = \frac{1}{n} \tag{7.28}$$

According to these considerations, the multihit survival functions of Eq. (7.14) correspond to the Γ distribution:
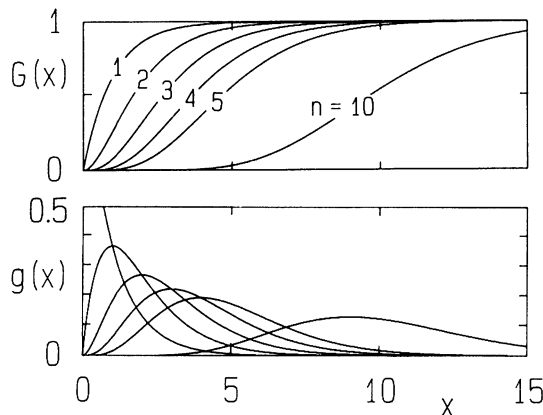
Figure 7.14. Densities and sum distributions for gamma distributions of order 1, 2, 3, 4, 5, and 10.

$$S(D) = 1 - G(x; n) = P(n; x) \tag{7.29}$$

where

$$x = aD \tag{7.30}$$

The survival function can be understood as a probability distribution of the inactivation dose D. The mean of the distribution is the mean inactivation dose $\overline{D}$ [see Eq. (7.2)]:

$$\overline{D} = \int_0^\infty D \, s(D) \, dD = \int_0^\infty S(D) \, dD \tag{7.31}$$

The variance of the inactivation dose is

$$\sigma^2 = \int_0^\infty (D - \overline{D})^2 \, s(D) \, dD = 2 \int_0^\infty DS(D) \, dD - \overline{D}^2 \tag{7.32}$$

The relative variance is

$$V = \frac{\sigma^2}{\overline{D}^2} \tag{7.33}$$

In the specific case of Eq. (7.14) one obtains, with the mean and the variance of the Γ distribution,

$$\overline{D} = \frac{n}{a} \quad \text{and} \quad \sigma^2 = \frac{n}{a^2} \tag{7.34}$$

and therefore,

$$V = \frac{\sigma^2}{\overline{D}^2} = \frac{1}{n} \tag{7.35}$$

The mean inactivation dose (or mean effect dose) $\overline{D}$ and the relative variance V of the dose–response relation have here been explained for the particular example of the n-hit process, that is, for the pure Poisson process. However, the considerations have more general validity. One can utilize the parameters D and V for any dose–effect relation.

The mean inactivation dose is not an unfamiliar concept for particular dose dependences. It equals the 50% survival dose D_{50} for a symmetrical dose–response relation; for exponential dose dependences it is identical with D_{37}. However, it is a universal parameter that applies to any dose–effect relation provided the relation can be extrapolated to doses where the effect probability approaches unity.

The relative variance of a dose–effect relation, or specifically a survival function, is an even more important parameter. It can serve as a quantitative measure for the deviation of the dependence from a threshold reaction. For a pure threshold reaction (that is, a step function) the relative variance V would be zero. For the multihit curves the relative variance equals the inverse of the hit number n [Eq. (7.35)]. The relative variance or its inverse, which is called relative steepness (6, 12), is therefore a generalization of the familiar concept of the hit number, which gives this concept general validity by making it independent of any particular model. Figure 7.15 exemplifies the general applicability of the parameters $\overline{D}$ and V. It is striking that the two most fundamental parameters of a distribution, the mean and the variance, are not very familiar concepts in the analysis of radiobiological dose–response relations. The reason is probably the convenience of using the conventional parameters [see for example (13)], which can be read off a graph and can be roughly estimated, even from crude data.

The relative variance of a dose–response relation is jointly determined by the statistical factors that are relevant to the response of the cells. The main factors are statistics of energy deposition, biological variability within the population, and the inherently stochastic response of the cell. It is in general not possible to separate the individual factors. An exception is the case of the simple exponential relation, for which the dominant factor can be the statistics of energy deposition.
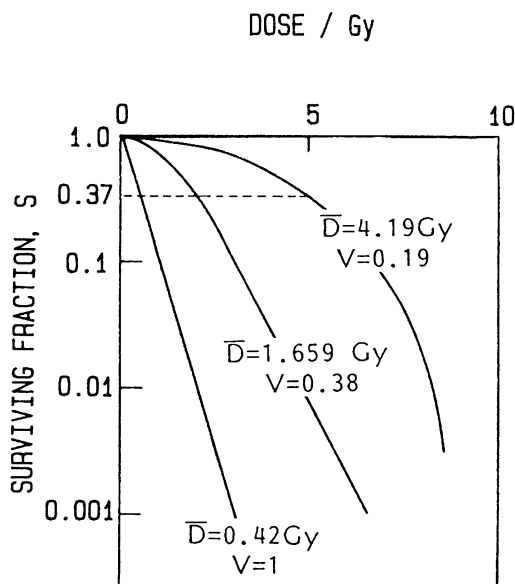

Figure 7.15. Schematic examples of different types of survival functions (adapted from Ref. 13). Parameters mean inactivation dose $\overline{D}$ and relative variance V are inserted. For comparison with observed survival functions for mammalian cells see Figure 7.6.

To explain a response function with small relative variance, one must invoke at least $1/V$ independent acts of energy deposition within the cell. No model involving a smaller mean hit number can lead to a response with this or a smaller value of the relative variance (6, 12, 14). The inferred number of events, the inverse of the relative variance, is merely a lower limit. The actual number of events relevant to the process will in general be larger because sigmoid dose–effect relations are codetermined by other statistical factors. Only an unknown part of the observed relative variance can then be ascribed to the statistics of energy deposition, and the number of energy deposition events must be larger than the theoretical limit. In subsequent sections it will be seen that the varying magnitude of the energy deposition events has an additional influence that works in the same direction.

The dose–effect relations in Figure 7.10 for the processes of Figure 7.4 illustrate the contribution of the statistics of energy deposition—including the spatial correlation of energy depositions—and the role of biological variability. It is evident that the nonuniformity of the reaction is dependent on the Poisson statistics, the "track structure," and the biological variability. Although the examples are highly schematic, they serve to demonstrate the complexity of the interplay of random factors that determines the dose–response relations. Simple relations are obtained only when the statistics of energy deposition is entirely dominant as a random factor; an example is the exponential survival functions obtained with very small objects (see Figure 7.3) or with densely ionizing radiation (see Figure 7.6).

In the subsequent sections the emphasis will be on the quantitative analysis of the one factor that is most characteristic for ionizing radiations, the statistics of energy deposition. It is difficult to assess the role of this factor in terms of complicated multihit processes. There have, nevertheless, been attempts to formulate threshold models in analogy to the target theory models. Such attempts will be surveyed after a section (7.3) that deals with fundamentals of microdosimetry. In a subsequent section simpler models will be considered that describe second-order processes of radiation action in terms of the actual microscopic distribution of energy deposition. There is good evidence from a variety of radiobiological investigations that ionizing radiations work on higher cells in a way that can broadly be termed a quadratic reaction. One can, accordingly, consider models that are sufficiently simple to remain tractable even if the highly complex patterns of energy deposition with ionizing radiations are taken into account.

7.3. CONCEPTS AND QUANTITIES OF MICRODOSIMETRY

7.3.1. Objective of Microdosimetry

The stochastic models of target theory postulate independent and equal random events of energy deposition. In reality, ionizing radiations impart energy to the exposed media in complex microscopic random patterns (Chapter 3). An approximate characterization of such patterns is afforded by the concept of linear energy transfer (LET). One pictures the charged particle tracks as straight lines with con-

stant rate of energy loss or as strings of ionizations regularly or randomly spaced along the trajectory of the particle with a density that corresponds to the LET, that is, to the mean energy loss of the particle per unit pathlength. This concept is widely used, but it has limited validity (see also Chapter 4). A more sophisticated approach was first developed by Lea (15). Later, when Rossi and his co-workers laid the theoretical and experimental foundations of microdosimetry (16–20), a coherent framework of concepts and quantities was created to quantify the statistics of energy deposition and the characteristic differences between various types of ionizing radiations.

The microscopic patterns of energy imparted by ionizing radiations to the exposed media can be determined by measurement or by computation. The most ambitious approach would be to determine all individual electronic alterations and their spatial coordinates. Although such an approach is not feasible, one can, as explained in Chapter 3, achieve the complex task of simulating the inchoate (initial) distribution of electronic changes produced by ionizing radiations within a specified volume. Any such distribution is a random configuration. Two identical exposures or random simulations would never result in equal spatial distributions of energy. Suitable parameters are required to characterize the random patterns. Ideally one would construct a hierarchy of characteristic parameters to express, with increasing degrees of sophistication, those properties of the distributions that determine the biological effectiveness of different radiations. Microdosimetry, in its general sense, is concerned with such characterization. In a conventional, more restricted sense it deals merely with certain quantities that are linked to the notion of energy concentration. These quantities are the specific energy z and the lineal energy y. They are considered first because they are suitable for the more elementary stochastic models of radiation biophysics.

When certain molecules are uniformly distributed in a solution, one can quantify their reactions in terms of equations that depend on their concentrations. The notion of concentration is not directly applicable when one considers small volumes that may contain only few of the molecules (see also Chapter 11). But even then the reaction kinetics remains comparatively simple because one can utilize the Poisson statistics of independently distributed molecules. The concentration remains the sole parameter that determines the distribution.

With ionizing radiations the situation is characteristically different. The energy imparted, and the subsequent radiation products such as free radicals, are not distributed in simple, uniform random patterns. Instead, they occur in clusters along the trajectories of charged particles (Chapters 3 and 4). Depending on absorbed dose and on the type and energy of the charged particles, the resulting inhomogeneity of the microdistribution can be very substantial. It is the reason that one cannot apply the notion of concentration directly. Measurements in randomly selected microscopic volumes will yield energy concentrations or concentrations of subsequent radiation products, which deviate considerably from their expectation values, and these variations depend in intricate ways on the size of the reference volumes, the magnitude of the doses, and the types of ionizing radia-

tions. Any quantitative description of radiation quality must account for the fluctuations of energy concentration, and it must therefore utilize concepts of probability theory.

The conventional quantities of microdosimetry are defined as concentrations in microscopic volumes. To account for the inapplicability of the simple concept of concentration, they must be treated as random variables.

7.3.2 Definition of Quantities and Distributions

7.3.2.1. Quantities

1. The energy imparted, ϵ, to a specified volume is equal to the energy of ionizing radiation incident on the volume minus the energy of ionizing radiation emerging from the volume.

A rigorous formulation (21) accounts also for possible changes of rest mass that are here disregarded.

2. The specific energy z is equal to the energy imparted divided by the mass of the reference volume.

The specific energy is the random analog of absorbed dose. Its expectation value is the absorbed dose in the specified volume. Its actual values can deviate substantially from the expectation value.

Specific energy has sometimes been called local dose. In those cases where one deals with a cell or a cell nucleus as reference volume, the term *cell dose* has been utilized. Such terms may be illustrative, but they are here avoided in order to exclude any confusion between the random variable, specific energy, and its mean value, the absorbed dose.

3. The lineal energy y is equal to the energy imparted divided by the mean diameter of the reference volume.

The term *mean diameter* stands for mean chord length under uniform, isotropic randomness. It is the average length of the straight-line segments that result when the reference volume is randomly traversed by straight particle tracks from a uniform, isotropic field. For a sphere the mean chord length is equal to two-thirds of the diameter. For any convex region the mean chord length is equal to four times the ratio of volume and surface (22, 23).

The quantity lineal energy has been conceived as a random analog to LET, and it is conventionally expressed in the same unit, keV/μm, as LET. In view of the analogy to LET, lineal energy is utilized with reference to single events only, that is, it refers to energy deposition due to one charged particle and/or its secondaries.

It is important for many considerations in microdosimetry to define an "energy

deposition event'' as energy deposition due to correlated particles. Energy deposition in a volume due to an α particle and its δ rays is one event. When an α particle misses a microscopic volume and injects several δ rays, the combined energy imparted belongs also to the same event, because the δ rays are associated particles. In principle, energy deposition by two or more charged particles belongs also to the same event if these particles are released by the same uncharged particle; however, this case is rarely of importance because uncharged particles do not tend to produce charged secondaries in close proximity. An exception is electrons of an Auger cascade.

The notion of energy deposition events is important in microdosimetry because, according to the definition, two energy deposition events are statistically independent. This is the condition for the application of the Poisson statistics; the occurrence of one event must neither increase nor decrease the probability for further events.

The three quantities ϵ, z, and y are closely related and largely equivalent. Subsequent considerations that are phrased in one of these variables can therefore be readily translated into another.

7.3.2.2. Dose-Dependent Distributions.

When a reference volume is repeatedly exposed to the same dose of a radiation, different values of specific energy z occur. With a sufficiently large number of exposures one obtains a probability distribution of the values of specific energy. Here $f(z; D) \, dz$ is the probability that a value of specific energy between z and $z + dz$ occurs in an exposure with absorbed dose D:

$$f(z; D) \, dz = \text{Prob}\{z \leq \underline{z} < z + dz \mid D\} \qquad (7.36)$$

The function $f(z; D)$ is the probability density (differential distribution) of specific energy z at absorbed dose D. The corresponding sum distribution is linked to the density:

$$F(z; D) = \int_0^z f(z; D) \, dz \qquad (7.37)$$

The distribution $f(z; D)$ contains a delta function at $z = 0$, that is, there is always a probability $F(0; D)$ for no energy deposition. This probability is vanishingly small at sufficiently high doses where many charged particles are expected to traverse the reference volume.

The probability distributions of specific energy or of the related microdosimetric quantities are fundamental concepts of microdosimetry, although their explicit shape is not often required. In pragmatic applications it is usually sufficient to utilize basic parameters of the distributions, which will be considered subsequently. In later sections certain diagrams will be employed to illustrate the distributions for different reference volumes, radiations, and absorbed doses.

7.3.2.3. Single-Event Distributions. Energy deposition in a specified microscopic volume occurs by independent charged particles and their correlated secondaries. The increments of specific energy in individual events can vary greatly, and the probability distribution of these event sizes in a specified volume is characteristic for a type of ionizing radiation.

The function $f_1(z)$ is the probability density of specific energy produced by individual events; that is, $f_1(z) \, dz$ is the probability that an energy deposition event produces a specific energy between z and $z + dz$.

The sum distribution of the event sizes is defined in analogy to Eq. (7.37):

$$F_1(z) = \int_0^z f_1(z) \, dz \tag{7.38}$$

In contrast to the dose-dependent distributions, there is no delta function at $z = 0$ in the single-event distribution $f_1(z)$.

7.3.3. Relations between Distributions

Microdosimetric distributions can be determined with detectors called Rossi counters. These are spherical devices with tissue-equivalent walls and an interior sensitive volume filled with tissue-equivalent gas. A central multiplication wire inside a suitable helix defines a multiplication region for the electrons that are liberated by ionizing radiations and are then collected. For the technical aspects of microdosimetry one may refer to the literature (18–20). In the initial development of microdosimetry, the dose-dependent distributions of specific energy were measured by multiple exposures of the counter to the same dose of a radiation. However, it was then realized that there is no need to measure the dose-dependent distributions, because they can be computed from distributions of the increments of specific energy produced by single events. Microdosimetric measurements need therefore be performed merely to obtain the single-event spectra. Figure 7.16 shows examples of such spectra for a spherical tissue region of diameter 1 μm and for different radiations.

In this diagram the dose-weighted distributions and their sum distributions are presented. They are defined as

$$d(y) = \frac{y f(y)}{\bar{y}_f} \qquad \bar{y}_f = \int_0^\infty y f(y) \, dy \tag{7.39}$$

with analogous formulas for the dose-weighted distributions of specific energy per event. The subscript f distinguishes the frequency average from the average of the dose-weighted distribution.

A relatively simple connection between the single-event distributions and the dose-dependent distributions exists because the individual events are statistically independent. Due to this statistical independence, the number of events at a spec-

SPECIFIC ENERGY / Gy
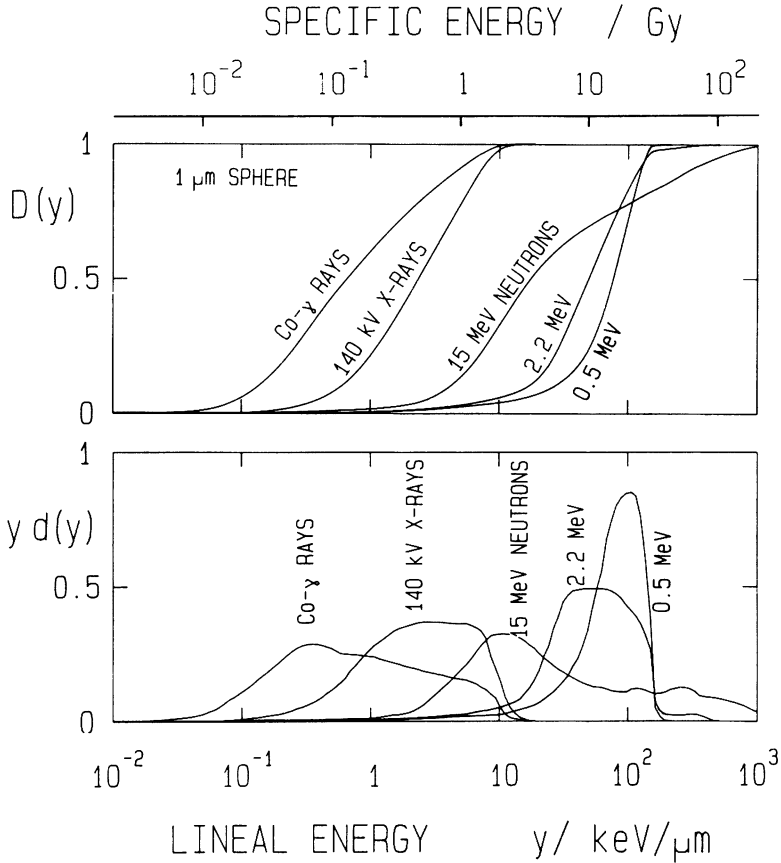
Figure 7.16. Distributions of lineal energy in spherical tissue regions 1 μm diameter exposed to various radiations. In the lower panel the distributions are represented as dose-weighted densities, $yd(y)$, relative to a logarithmic scale of lineal energy y. These spectra determine the fraction of absorbed dose delivered per unit logarithmic interval of lineal energy. In the upper panel the corresponding sum distributions $D(y)$ are given; they specify the fraction of energy delivered by events up to lineal energy y. On top of the upper panel an additional abscissa is given for the specific energy z. Relative to this scale the curves in the lower panel are the weighted densities $zd_1(z)$ of specific energy in single events; the curves in the upper panel are the sum distributions $D_1(z)$ of specific energy in single events. Data from Refs. 14, 27, 28.

ified dose follows the Poisson distribution (Section 7.2). The probability for exactly ν events is

$$p(\nu) = \exp(-n)\,\frac{n^{\nu}}{\nu!} \tag{7.40}$$

where n equals $D/\bar{z}_f$, and $\bar{z}_f$ is the mean specific energy produced per event:

$$\bar{z}_f = \int_0^\infty z f_1(z) \, dz \tag{7.41}$$

The formulas for the distributions of specific energy are more complicated than Eq. (7.40) because they do not deal with a simple Poisson process that is characterized by the identity of events. Individual energy deposition events can impart greatly different energies to the target volume. For this reason one speaks of a mixed (or compound) Poisson process. If a random variable results from a mixed Poisson process, its value depends on the number of events that have taken place and on the randomly varying size of the events. The equation for the specific energy at a specified dose is

$$f(z; D) = \sum_{\nu = 0}^\infty p(\nu) f_\nu(z) \tag{7.42}$$

where $p(\nu)$ is the probability for exactly ν events, and $f_\nu(z)$ is the probability distribution of specific energy that results when exactly ν events occur. The latter distribution is obtained by the operation of convolution, which is fundamental in probability theory.

When a random variable is the sum of two independent random variables, its distribution is the convolution of their distributions. The specific energy from two events is the sum of the two statistically independent increments produced in these events, and the probability distribution of specific energy for exactly two events is therefore

$$f_2(z) = \int_0^z f_1(z - s) f_1(s) \, ds \tag{7.43}$$

A straightforward extension gives the recursion formula that links the distribution for exactly ν events with that for $\nu - 1$ events:

$$f_\nu(z) = \int_0^z f_{\nu - 1}(z - s) \, f_1(s) \, ds \tag{7.44}$$

In view of the importance of the operation of convolution, one uses an abbreviated notation instead of the explicit integral. Equations (7.43) and (7.44) read, using this notation,

$$f_2(z) = f_1(z) * f_1(z) = f_1^{*2}(z)$$
$$f_\nu(z) = f_{\nu - 1}(z) * f_1(z) = f_1^{*\nu}(z) \tag{7.45}$$

Instead of using the recursion formula (7.44), it is economical to compute first the convolutions that correspond to powers of 2:

$$f_2(z) = f_1(z) * f_1(z) \tag{7.46}$$

$$f_4(z) = f_2(z) * f_2(z)$$

$$\vdots \tag{7.47}$$

and then to perform appropriate convolutions of these distributions to reach any desired number. For example, the distribution for exactly 100 events is obtained as

$$f_{100}(z) = f_{64}(z) * f_{32}(z) * f_4(z) \tag{7.48}$$

In actual computations a further refinement is utilized (24–26). Its consideration will facilitate some of the developments in subsequent sections.

If two exposures are applied, each with dose D, the resulting specific energy is the sum of the independent contributions of the first and the second exposure. In other words, the distribution of specific energy for the dose $2D$ is the convolution of the distributions for dose D:

$$f(z; 2D) = f(z; D) * f(z; D) \tag{7.49}$$

Repeating the process, one can readily reach the distribution for the fourfold dose, the eightfold dose, and so on. This implies that a distribution of specific energy for high doses can be obtained from the distribution for low doses. For very low doses, however, one can give the distribution directly in terms of the single-event distribution and of a delta function at $z = 0$. If a dose d is small compared to $\bar{z}_f$, the average specific energy in one event, it is very likely that no event takes place, that is, the distribution contains a delta function at $z = 0$ with a coefficient close to 1. With small probability, $d/\bar{z}_f$, one event occurs, and this corresponds to the single-event distribution with coefficient $d/\bar{z}_f$. The probability for two or more events is proportional to the square of $d/\bar{z}_f$, that is, to a small number that can be disregarded. For a small dose d one can thus approximate the distribution of specific energy by the equation

$$f(z; d) = \left(1 - \frac{d}{\bar{z}_f}\right) \delta(z) + \frac{d}{\bar{z}_f} f_1(z) \tag{7.50}$$

To compute the distribution for a larger dose D, one chooses a small submultiple, $d = D/2^N$, and derives the desired distribution by N successive convolutions. In this way one can obtain the distribution for a mean value of 100 events by 14 convolutions starting with the dose that corresponds to only 0.0061 events on the average. By this method one generates sets of distributions for doses increasing by factors of 2. Figures 7.17 and 7.18 give such sets of distributions and sum distributions for sparsely ionizing radiations and densely ionizing radiations.
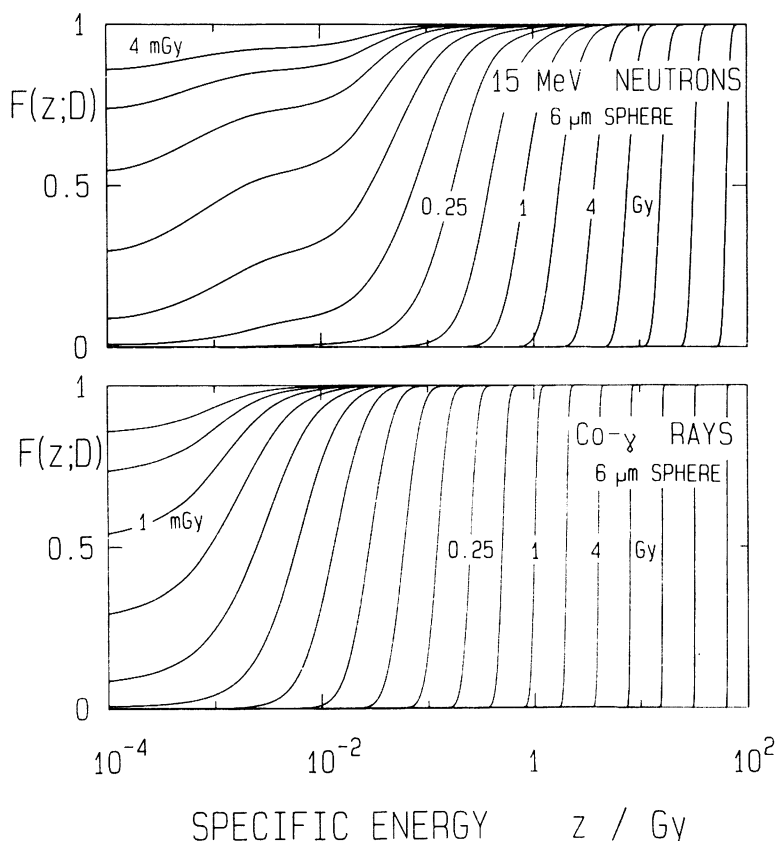
Figure 7.17. Sum distributions $F(z; D)$ of specific energy in a unit density tissue sphere of 6 μm diameter exposed to different doses of Co γ rays and 15-MeV neutrons. The distributions are calculated by the algorithm of successive convolutions (26).

A single-event distribution can extend over an extremely broad range of energy imparted. As seen, for example, in the spectrum for 15-MeV neutrons (Figure 7.16), possible values extend from a few electronvolts to several hundred kilo-electronvolts. Such distributions can be displayed on a logarithmic scale. Fast algorithms have been formulated that perform the convolution directly on the logarithmic scale (24, 26); they are more practical than the use of the fast Fourier transform, which necessitates linear scales.

7.3.4. Moments of Microdosimetric Distributions

In applications of microdosimetry one rarely requires the explicit distributions of specific energy. It is frequently sufficient to use certain parameters that characterize these distributions. Most important among such parameters are the moments of the
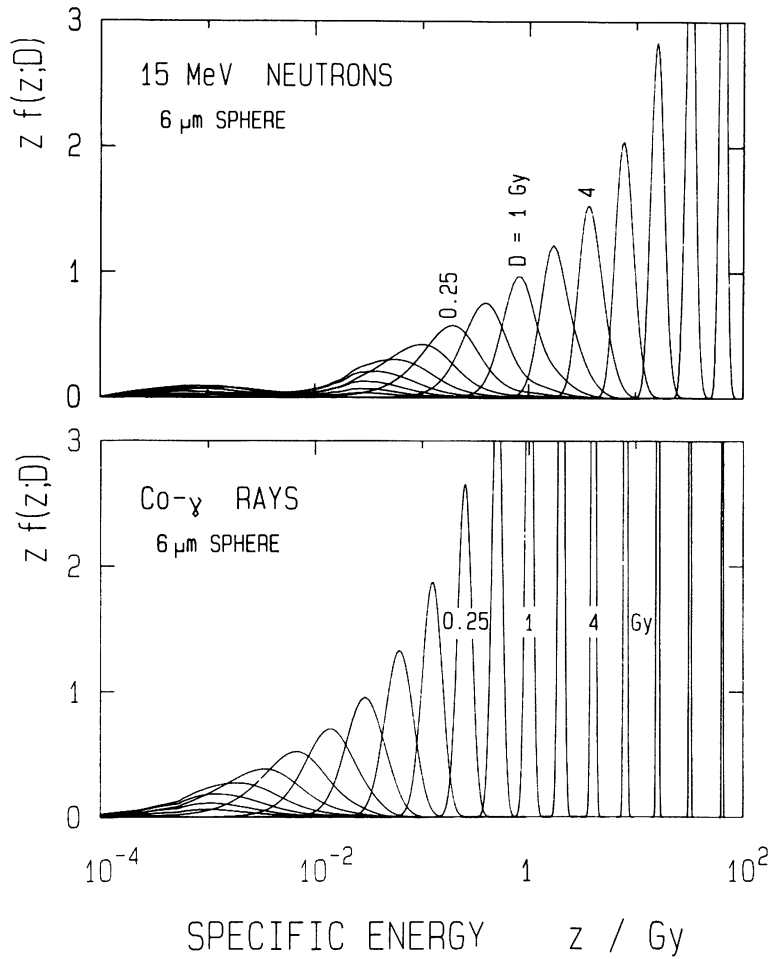
Figure 7.18. Densities $z f(z; D)$ of specific energy that correspond to the sum distributions in Figure 7.17.

distribution. The moments are the expectation values of the integer powers of the random variable. The first moment is the mean value; the second moment is closely related to the variance. The moments can be derived either for the single-event spectra or for the dose-dependent spectra, and it will be seen that they are interrelated.

The moments for the single-event spectra are

$$\overline{z_1^n} = \int_0^\infty z^n f_1(z) \, dz \tag{7.51}$$

The index 1 indicates that the quantities correspond to the occurrence of exactly one energy deposition event in the reference region. To adhere to the conventional notation, the symbol $\bar{z}_f$ is used instead of $\bar{z}_1$.

In contrast to the moments of the single-event distributions, the moments of the distributions $f(z; D)$ depend on absorbed dose. They are defined as

$$\overline{z^n} = \int_0^\infty z^n f(z; D) \, dz \tag{7.52}$$

The moments of the dose-dependent distributions can be expressed in terms of the moments of the single-event distribution (24–26):

$$\bar{z} = \int z f(z; D) \, dz = D$$

$$\overline{z^2} = \int z^2 f(z; D) \, dz = \frac{\overline{z_1^2}}{\bar{z}_f} D + D^2$$

$$\overline{z^3} = \int z^3 f(z; D) \, dz = \frac{\overline{z_1^3}}{\bar{z}_f} D + \frac{3\overline{z_1^2}}{\bar{z}_f} D^2 + D^3 \tag{7.53}$$

$$\cdot \; \cdot \; \cdot$$

$D/\bar{z}_f$ is the mean number of events at absorbed dose D. The mean specific energy per event, $\bar{z}_f$, is the inverse of the event frequency per unit absorbed dose.

The relation for the second moment of the dose-dependent distribution is of special importance in biophysical considerations of second-order processes, that is, of reactions that depend on the square of the specific energy so that their yield is proportional to the expectation value of the square of specific energy. Because of its special pragmatic importance, the relation for the second moment is here derived, although reference is also made to the more general derivation of the relations (7.53) for all moments (24–26).

When a random variable such as z is the sum of two statistically independent random variables, say x and y, its variance is the sum of the variances of the individual variables. This fundamental relation is readily derived. For any random variable one has

$$\sigma^2 = \overline{(z - \bar{z})^2} = \overline{z^2 - 2z\bar{z} + \bar{z}^2} = \overline{z^2} - \bar{z}^2 \tag{7.54}$$

For the second moment of the sum of two independent random variables one obtains (with $\overline{xy} = \bar{x}\,\bar{y}$, due to the statistical independence)

$$\overline{z^2} = \overline{(x + y)^2} = \overline{x^2 + 2xy + y^2} = \overline{x^2} + \overline{y^2} + 2\,\bar{x}\,\bar{y} \tag{7.55}$$

The square of the mean is

$$\bar{z}^2 = (\overline{x + y})^2 = \bar{x}^2 + \bar{y}^2 + 2\,\bar{x}\,\bar{y} \tag{7.56}$$

Therefore,

$$\sigma_z^2 = \overline{z^2} - \bar{z}^2 = \overline{x^2} - \bar{x}^2 + \overline{y^2} - \bar{y}^2 = \sigma_x^2 + \sigma_y^2 \tag{7.57}$$

The variances of specific energy due to two dose increments applied successively are additive, and the variance of specific energy is, therefore, proportional to absorbed dose:

$$\sigma_z^2(D) = kD \tag{7.58}$$

The constant k can be obtained from the approximation [Eq. (7.50)] for a small dose d:

$$\bar{z} = d \quad \text{and} \quad \overline{z^2} = \frac{d}{\bar{z}_f}\,\overline{z_1^2} = \frac{\overline{z_1^2}}{\bar{z}_f}\,d \tag{7.59}$$

Utilizing Eq. (7.54) and the symbol $\bar{z}_d$ for the mean of the dose-weighted distribution [see Eq. (7.39)], one has

$$\sigma_z^2 = \bar{z}_d\,d - d^2 \quad \text{where } \bar{z}_d = \frac{\overline{z_1^2}}{\bar{z}_f} \tag{7.60}$$

The quadratic term d^2 is an inaccuracy due to the omission of multiple events in Eq. (7.50); the resulting fractional error $d/\bar{z}_d$ of the variance vanishes for sufficiently small values of d. The important formula for the variance of z agrees with Eq. (7.53):

$$\sigma_z^2 = \bar{z}_d D \tag{7.61}$$

It is essential for models of cellular radiation action that postulate a dependence of the effect on the square of the energy concentration (see Section 7.4.2).

7.3.5. Illustration of Microdosimetric Data

In Chapter 3 examples and graphic representations of charged particle tracks are given. Such descriptions provide the information that is essential for an understanding of microdosimetric spectra and for an appreciation of the substantial differences of local energy densities produced by sparsely and densely ionizing ra-
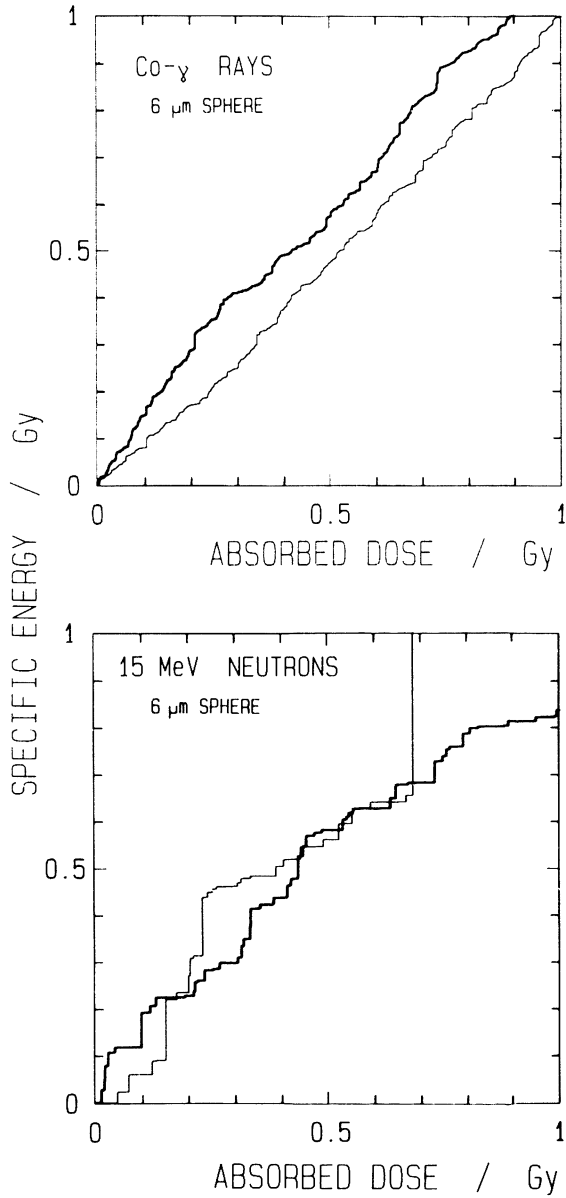
Figure 7.19. Two random paths that represent the stochastic sequence of events of energy deposition in a 6-μm tissue sphere exposed to Co γ rays and 15-MeV neutrons.

diations. When one considers distributions of specific energy or of lineal energy, one replaces the detailed information on the spatial positions of energy transfers by a description that contains some of the information implicitly. It is useful to illustrate the distributions by a series of diagrams.

Figure 7.19 refers to spherical tissue volumes with the approximate dimensions of the nucleus of a mammalian cell. Measured single-event spectra of specific energy produced by ^{60}Co γ rays and by 15-MeV neutrons in such spheres are utilized to create random simulations of the accumulation of specific energy in the sites. Each panel gives two sequences of the random process from dose zero up to 1 Gy. The statistical fluctuations are smaller for the sparsely ionizing γ rays; nevertheless, one notes that at least in one of the two random sequences (heavy line), the deviation of specific energy from its mean, the absorbed dose, happens to be sizable even at the dose of 1 Gy. Therefore, one cannot disregard the microdosimetric fluctuations of energy deposition entirely even if one deals with sparsely ionizing radiation and with the entire nucleus of the cell at the relatively high dose of 1 Gy.

The random steps of energy deposition are far larger and correspondingly less frequent with 15-MeV neutrons. For example, one of the two random sequences contains at its end (only partially represented in the diagram) an increment of spe-
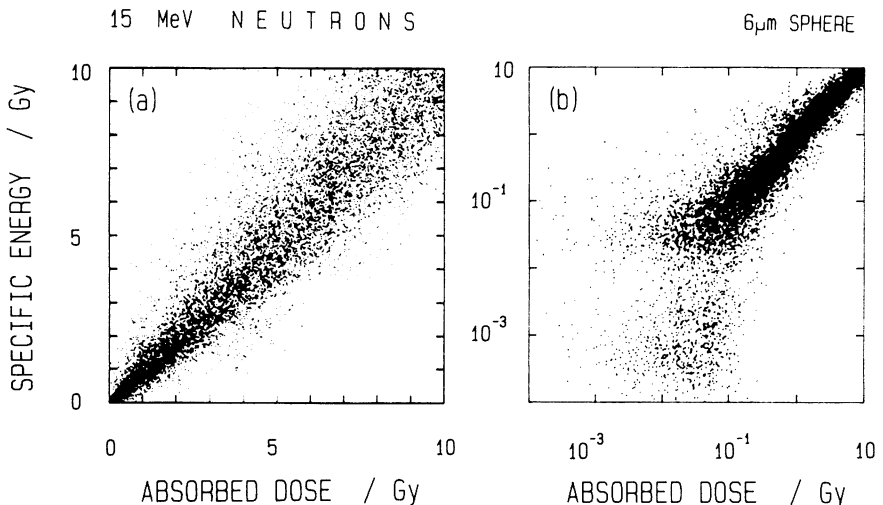
Figure 7.20. Scatter diagrams of the distribution of specific energy at specified absorbed doses in spherical tissue regions 6 μm diameter exposed to 15-MeV neutrons. In analogy to Figure 7.19 a linear scale of absorbed dose and specific energy is used in the left panel. The right panel uses logarithmic scales; it demonstrates that the relative fluctuations of specific energy decrease at larger doses. In each diagram a large number of absorbed dose values uniformly distributed on the abscissa scale is used. Each dot represents the value of specific energy from a random simulation of the exposure with the chosen value of absorbed dose.

cific energy of about 0.5 Gy. A carbon recoil of 1 MeV can produce in the nucleus of the cell an increment of specific energy in excess of 20 Gy; although this is a rare event, it illustrates the enormous range of increments of specific energy caused by energetic neutrons.

A small number of random paths can give a rough indication of the process of energy accumulation in a microscopic structure. For a quantitative evaluation one needs a large number of simulations. A superposition of many random paths would not provide a readable diagram. To obtain a better representation, one can consider varying values of absorbed dose and derive for each of these a random value of
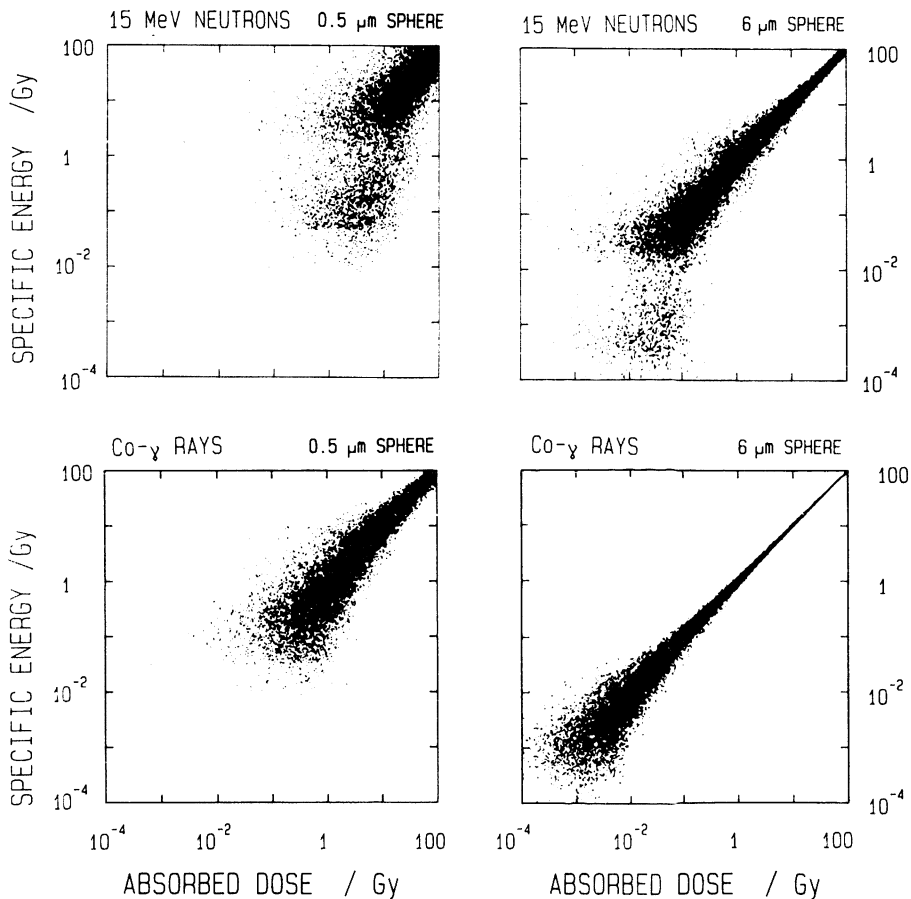
Figure 7.21. Scatter diagrams for a comparison of z distributions in small sites and in sites that correspond roughly to the diameter of the nucleus of a cell (6 μm). Here and in Figure 7.22 each panel contains 4000 simulations per decade of D. The number of plotted points is considerably less at low doses because the events with $z = 0$ are not visible.

the specific energy. In this way one obtains a cloud of points in a $D–z$ diagram, as represented in Figure 7.20 for the 15-MeV neutrons. In the comparison with the right panel of Figure 7.19, one must note that the diagram is extended to an absorbed dose of 10 Gy. In the simulation 10,000 points are chosen with values of absorbed dose equally distributed between 0 and 10 Gy.

The diagrams of Figure 7.19 and the left panel of Figure 7.20 show that the fluctuations are largest at the highest doses. However, the absolute magnitude of the fluctuations is not the relevant parameter. In most applications the relative fluctuations are more meaningful. To judge such deviations and, at the same time, to obtain a diagram that covers a vastly larger dose range with sufficient accuracy, one can utilize a logarithmic representation as in the right panel of Figure 7.20. Such representations are also utilized in Figures 7.21 and 7.22 where the distri-
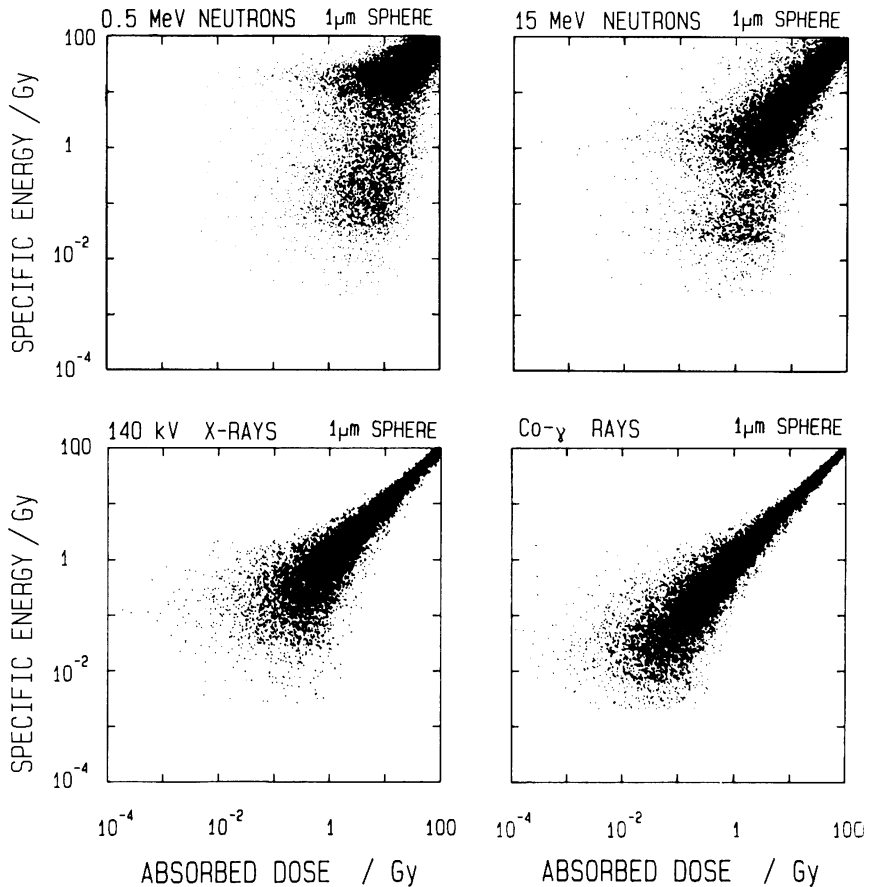
Figure 7.22. Scatter diagrams as in Figure 7.21 but for a comparison of 140-kV X rays, Co γ rays, 0.55-MeV neutrons, and 15-MeV neutrons for a spherical tissue site 1 μm diameter.

TABLE 7.1. Frequency Average $\bar{z}_f$ and Dose Average $\bar{z}_d$ of Specific Energy z (Gy) Produced by Single Events in Spherical Tissue Regions[a]

Diameter of Spherical Region, d (μm)		^{60}Co γ Rays	Neutrons	
			0.43 MeV	15 MeV
12	$\bar{z}_f$, 0.0004		0.018	0.016
	$\bar{z}_d$, 0.0011		0.033	0.092
5	$\bar{z}_f$, 0.003		0.24	0.10
	$\bar{z}_d$, 0.008		0.32	0.75
2	$\bar{z}_f$, 0.02		2.0	0.63
	$\bar{z}_d$, 0.07		2.8	4.9
1	$\bar{z}_f$, 0.09		10	2.6
	$\bar{z}_d$, 0.37		14	20
0.5	$\bar{z}_f$, 0.56		48	11
	$\bar{z}_d$, 2.2		62	82

[a]Values obtained by interpolation from a variety of measured and calculated data (20). With the units Gy, keV, and μm one has for spherical regions the following relations between specific energy z, lineal energy y, and energy imparted ϵ: $z = 0.204 y/d^2$; $y = 4.9 z d^2$; $y = 1.5\epsilon/d$; $z = 0.306\epsilon/d^3$. The event frequency per unit dose is $\bar{z}_f^{-1}$.

butions are compared for different radiation qualities and for different site sizes. To create these diagrams, the chosen values of absorbed dose were equally distributed on the logarithmic scale. There are few points at the small doses where the value 0 of specific energy becomes very probable; points that correspond to the absence of any absorption event do not appear on the diagram.

Although the scatter diagrams can visualize the magnitude of the fluctuations of specific energy for different radiation qualities, for different site sizes, and for different doses, they contain more information than is usually required in applications of microdosimetric data. Event frequencies and mean event sizes are more frequently utilized. Table 7.1 illustrates the magnitude of these quantities in typical cases.

7.4. MICRODOSIMETRIC MODELS OF CELLULAR RADIATION ACTION

7.4.1. Threshold Models and Their Extension

When a new technique has been developed, it is natural to seek improvements of earlier approaches. Accordingly, certain notions of target theory were revived and extended after the concepts of microdosimetry had been introduced and microdosimetric data had become available.

The target theory approaches, such as the multihit and multitarget models, were unrealistic in postulating events of equal energy deposition in certain assumed target regions. Microdosimetric data permit a more accurate description. If one wishes to retain the general concepts of the multihit models, one can replace them by threshold models in terms of microdosimetry. Such threshold models were considered during the earlier stages of the development of microdosimetry and were then replaced by models that were more meaningful and in better agreement with radiobiological findings. These more pragmatic models are dealt with in the subsequent section. A brief consideration of the threshold models is, nevertheless, required to put into perspective the instances where earlier approaches are retraced, usually with somewhat different and not always with clearly defined terminology.

The essence of the threshold models is the postulate of a sensitive site in the cell with a critical threshold of energy deposition for the cellular effect (for example, loss of proliferative ability) to occur. Although a model of this type is an abstraction, it can lead to certain firm conclusions.

In the simplest approach one assumes that the sensitive site is a sphere of specified diameter and that the critical threshold of specific energy in the site is z_c. The survival relation is then

$$S(D) = F(z_c; D) \qquad (7.62)$$

where $F(z; D)$ is the sum distribution of specific energy for the radiation in question and for the specified diameter [see Eq. (7.37)]. While Eq. (7.62) is the analog of Eq. (7.29), it applies to a compound Poisson process, that is, to events of energy deposition of randomly varying magnitude. The solutions are therefore more complicated than those for the multihit models; however, as explained in the preceding section, they are readily computed from single-event spectra. For a diameter of 6 μm and for 15-MeV neutrons and Co γ rays, the functions are given in Figure 7.17. Replotting these data versus absorbed dose rather than specific energy, one obtains the dependences in Figure 7.23. They would be the dose–effect relations if the cell nucleus were the critical site and if it were to react at a sharp threshold of specific energy.

The relative variance of these dose dependences is substantially less than typical values observed in cell inactivation studies with γ rays or fast neutrons (see Figure 7.6). Either the critical targets in the cell must therefore be smaller, so that the fluctuations of energy deposition are larger, or other stochastic factors (that is, biological variability and the inherent stochastic response of the cell) must contribute largely to the observed variance of the response. Probably both conditions apply.

Considering the statistics of energy deposition as the only relevant factor, one could determine the site diameter, which yields, for a postulated threshold reaction, the relative variance of an observed cell survival function. Figure 7.24 gives the solutions for a target diameter of 1 μm. Cellular survival data either fit into the set of these curves (see Figure 7.6) or they have larger relative variances. For a
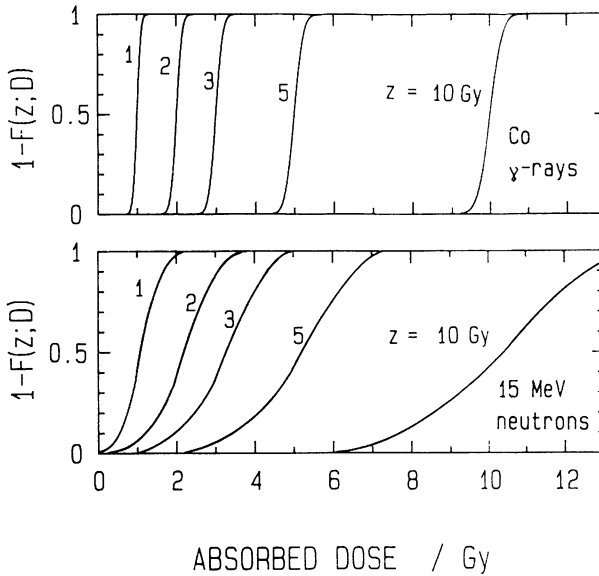
Figure 7.23. Probabilities to exceed a critical value z of specific energy in a spherical tissue site 6 μm diameter. The data correspond to those of Figure 7.17.

smaller target size the relative variances would increase; that is, they would be inconsistent with experimental observations. Any model based only on the reaction of a single target smaller than 1 μm must therefore be rejected. Equally excluded are models that invoke a multiplicity of independent targets of smaller size. On the other hand, one may postulate a larger target or a multiplicity of interdependent small targets spread over a larger region, and one can then obtain dose depen-
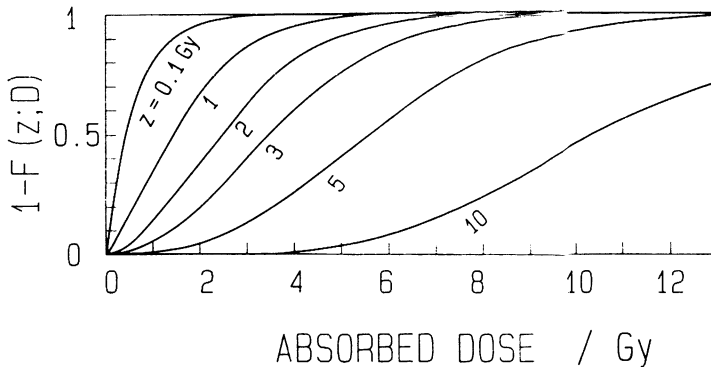

Figure 7.24. The probabilities to exceed a critical value z of specific energy in spherical tissue sites 1 μm diameter exposed to X rays.

dences with small relative variances. If the model yields a dose dependence with too little relative variance, it is still consistent with the observations since part of the observed variance can be ascribed to additional random factors not linked to the statistics of energy deposition. This argument is analogous to the earlier considerations of the multihit model. The main conclusion is that a threshold-type argument in terms of microdosimetry can provide a lower bound for the size of the gross sensitive region; the actual dimension will usually be larger.

The argument is often misinterpreted. The preceding considerations cannot exclude models that postulate smaller targets—for example, localized damage in the DNA—as the lethal event in the cell. However, to explain a nonexponential dose dependence (relative variance < 1), the model must invoke additional mechanisms that extend over longer ranges. Thus, one could postulate a dose-dependent inhibition or overload of repair. But there is, at present, no experimental evidence for a reduction of the repair capacity or the rate of repair at doses of a few gray which are relevant to cellular radiation effects. Reduced efficiency of repair or enhanced misrepair are apparent at elevated doses of sparsely ionizing radiations and at all doses of densely ionizing radiations, but they can be understood in terms of the greater proximity of sublesions of DNA and the resultant failure of DNA repair. A simple example would be two neighboring single-strand breaks on opposing strands of DNA, which interfere with excision repair. Such interference with repair due to spatial proximity of sublesions is, in a somewhat loose terminology, included in the general notion of the "interaction" of sublesions. Microdosimetric analysis provides information on the magnitude of distances involved; it cannot, by itself, identify the molecular nature of the processes.

Threshold considerations provide general conclusions without actual commitment to the reality of a threshold. Biological objects do not exhibit defined thresholds in terms of energy deposition in certain target structures. More complex models have therefore been considered in the past, and they have been revived from time to time.

These approaches postulate a spherical target region, sometimes the cell nucleus, sometimes a smaller structure. The effect probability at a certain dose is the integral of the effect probabilities for all possible values of specific energy in the target volume. Formally this is written as

$$E(D) = \int_0^\infty E(z)f(z; D)\, dz \qquad (7.63)$$

If one postulates this relation and assumes that one knows, with sufficient precision, not only the microdosimetric distribution $f(z; D)$ but also the dose–effect relation $E(D)$, one can invert Eq. (7.63) and deduce the response function $E(z)$. The knowledge of this function is then expected to elucidate underlying mechanisms or, at least, to make possible a prediction of the efficiency of other types of ionizing radiations for which the microdosimetric distributions are known.

The approach may appear attractive. However, there are hidden assumptions and hidden difficulties. First, the selection of the reference target is uncertain. The only reasonable choice may be the entire nucleus of the cell. However, for sparsely ionizing radiations it is apparent from Figure 7.18 that the distributions $f(z; D)$ are narrow and that, accordingly, the function $E(z)$ is not substantially different from the observed dose–effect relation $E(D)$. The additional insight is then minimal. The fluctuations of specific energy in the entire nucleus of the cell are simply too small for sparsely ionizing radiations to play a major role at doses of one or several grays. A second weakness of the approach is an inherent assumption that underlies Eq. (7.63). It is assumed that the effect probability depends merely on the specific energy in the reference region; no account is taken of the fact that equal values of specific energy may be associated with different distributions of energy imparted within the target region. In certain extreme cases the differences can be very substantial; it is then not justified to expect the same efficiency of the radiations at equal values of z in the nucleus of the cell. The standard example is that of electrons of very short range. A 1-keV electron deposits its energy very locally in the nucleus of the cell and can thus be quite effective. This has been substantiated by various comparative studies of the effects of soft X rays and of energetic sparsely ionizing radiations (30, 31). The cellular effects of the low-energy electrons are found to be comparable to or even larger than those of higher energy electrons, although the latter produce larger values of specific energy in the cell nucleus as a whole. The effect on the cell can, therefore, not be a mere function of the specific energy in the nucleus; it depends in an insufficiently understood way on the spatial microdistribution of energy.

Further conclusions are obtained from experiments by Rossi et al. (32–34) with correlated pairs of protons or deuterons. In these experiments pairs of particles traverse mammalian cells with small lateral separations of variable magnitude. By comparison to single particles of twice the stopping power, it is found that a lateral separation of only 0.1 μm causes an appreciable reduction of the effect. On the other hand, nearly the same energy is deposited in the nucleus under the two conditions (left and central panel of Figure 7.25). Therefore, the energy in the nucleus of the cell cannot be the parameter that determines the probability of the effect on the cell.

Even for the same radiation Eq. (7.63) need not be valid. At a larger value of absorbed dose a specified value of z will more likely arise from several events than from one event. If it is produced by several events, the energy will tend to be more loosely spaced (as indicated in the diagram of Figure 7.26), and the effectiveness will then be reduced. The temporal distribution of events is an additional factor that can determine the extent of DNA repair and thus the magnitude of the observed cellular effect.

The main weakness of the approaches considered in the present section is the multiplicity of assumptions and parameters. Radiobiological data are not usually of sufficient precision to permit complex numerical analysis. Simpler approaches are required to test basic principles of the action of ionizing radiations on the cell.

SINGLE IONS 66 keV/μm   PAIRED IONS 33 keV/μm   SINGLE IONS 33 keV/μm
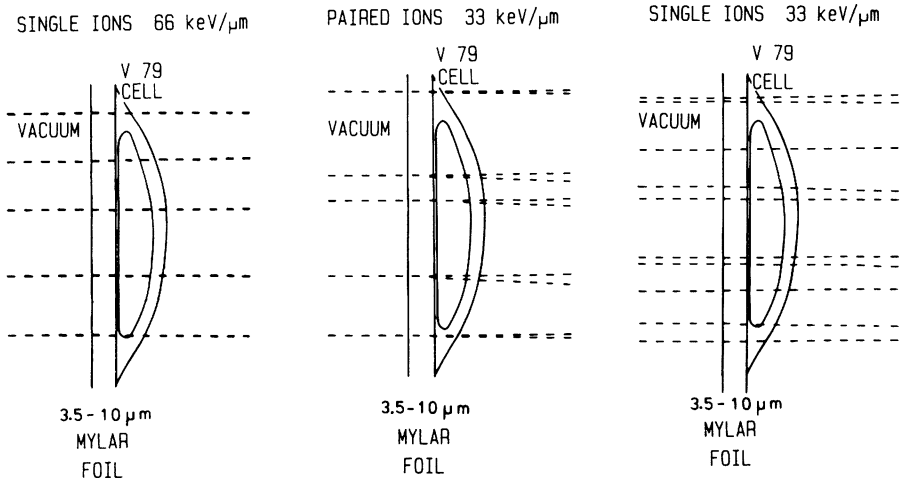
Figure 7.25. Schematic diagram to indicate the result of the molecular-ion beam experiments (adapted from Ref. 33). Protons with linear energy transfer 66 keV/μm (left panel) are substantially more effective at a given dose than pairs of protons of half the stopping power traversing the nucleus of the cell simultaneously with lateral distance on the order of 0.1 μm (center panel). Uncorrelated protons of 33 keV/μm (right panel) are still somewhat less effective.

The subsequent section deals with one particular approach which, in spite of its restricted validity, has led to tangible insights.

7.4.2. Site Model of Dual Radiation Action

7.4.2.1. General Considerations. In the preceding section notions of target theory have been reconsidered within the framework of microdosimetry. This section deals in more detail with one particular approach, the application of microdosimetry to a second-order process. The objective of the treatment is to bring out essentials.
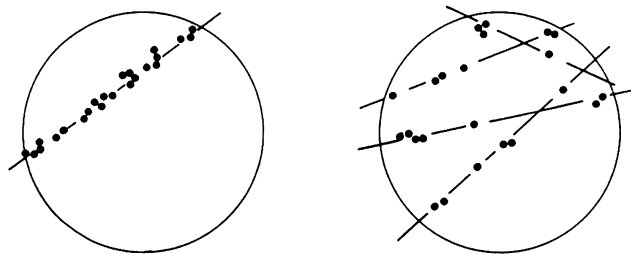
Figure 7.26. Schematic diagram to indicate that the distances between energy transfers tend to be smaller for one track segment in the site than for several track segments in the site with the same total energy transfer.

When a charged particle traverses the cell, it distributes its energy, with a degree of randomness, to an array of sensitive structures. Even if one were to assume a multiplicity of cells subjected to the same microscopic configuration of energy deposition, one could not expect equal effects. The cell responds somewhat randomly to the initial electronic alterations produced by ionizing particles, and any quantitative description of the action of ionizing radiations must therefore be of statistical nature (see also Chapter 6).

The immediate consequence is the rejection of any threshold model of radiation action. As indicated in the preceding section, threshold considerations may nevertheless be useful in the derivation of general conclusions. They can serve to exclude certain modes of radiation action. As a pragmatic description, however, a threshold model must fail. In fact, the models have been tried and rejected in earlier attempts to apply microdosimetric data—for example, to the analysis of cataracts (35) caused by neutrons or X rays or to the analysis of mutations in maize (36) produced by these radiations.

As also pointed out in the preceding section, one can postulate general empirical response functions for specific energy in certain targets [see Eq. (7.63)] and then try to derive from a set of observations, with different radiation qualities and different doses, those parameters that appear most consistent with the experiments. The approach has so many degrees of freedom that it will always yield solutions; in fact, it will usually give a wide choice of solutions that fit the data equally well. Meaningful conclusions will therefore be minimal.

A more pragmatic procedure is to start with narrow assumptions and to test them against available experimental evidence. By a stepwise process of modifications better descriptions may be attained. Unlike other models, the dual-action model was originally (29) based on assumptions narrow enough to permit conflicts with observations.

Many dose–effect relations for sparsely ionizing radiations can be adequately described by a linear-quadratic function in absorbed dose or by an exponential function that contains a linear-quadratic term in absorbed dose. The quadratic term tends to predominate with sparsely ionizing radiation, and the linear term becomes more important for densely ionizing radiations. Even in certain experimental investigations [for example, radiation-induced cataracts (37)] where the dose–effect relation, in itself, is hardly amenable to a numerical description, the relative biological effectiveness–dose relation is indicative of an underlying process that appears to be quadratic for sparsely ionizing radiations and linear for densely ionizing radiations. Various radiobiological observations are consistent with a proportionality of the relative biological effectiveness (RBE) of neutrons to the inverse square root of the neutron dose (14, 29). Some of the early observations have motivated a quantitative analysis of second-order processes in terms of microdosimetry. Results of subsequent studies have been the most tangible result of insights obtained or of experiments suggested by the microdosimetric analyses.

Lea (15) may have been the first to attempt a general treatment of second-order processes in radiation biology. He was concerned with the production of chro-

mosome aberrations by pairs of sublesions. His essential arguments were later rephrased in terms of microdosimetry.

7.4.2.2. Notion of Concentration Applied to Nonhomogeneous Distributions. A

second-order process due to chemical agents is a simple matter when one deals with homogeneous kinetics. The yield is proportional to the square of the concentration of the reactant or to the product of the concentrations of two reactants. A condition for the simple relation is that effects of saturation or depletion can be disregarded.

With ionizing radiations a second-order process cannot result in a purely quadratic dose–response relation. The reason is the failure of the notion of concentration of energy or of any subsequent radiation products. The irregular microscopic pattern of energy deposition produced by the random appearance and random behavior of charged particles and their secondaries precludes the naive application of the notion of concentration. Conventional microdosimetry is nevertheless an attempt to apply the notion of concentration, but in a more general sense. One measures concentrations of energy over specified microscopic regions, the reference volumes of microdosimetry (see also Chapter 4). Choosing a certain scale (that is, the diameter of a spatial probe, the reference region), one samples the exposed medium, and a probability distribution of concentrations in the probe is obtained. The random variable specific energy takes the place of concentration. Probability distributions are used instead of single-valued parameters.

A second-order process results from the pairwise combination of reaction partners. If the reaction partners can diffuse sufficiently fast and if they live sufficiently long, they may react over large distances. If they are short-lived or have fixed positions, they react only over small distances. A simple example mentioned in the last section is that of two adjacent single-strand breaks on opposite strands of the DNA; with excision repair they can lead to misrepair. In general, reaction partners may have a high probability to interact if they are created a short distance apart; they have a reduced reaction probability if they are created further apart. A mathematical description is given in Section 7.5. The present section deals with a simple approximation that is not unlike the arguments utilized by Lea.

The essence of the approach is to postulate initial radiation products (sublesions) whose yield is proportional to energy imparted and that can react pairwise. A fixed reaction probability is assumed between sublesions less than a certain distance apart. Interactions beyond this distance are disregarded. On the basis of microdosimetric data for different radiations, such assumptions can be translated into dose–response relations. One can then try to identify those sizes of the reference region that agree best with experimental observations for substantially different radiation qualities. This approach is chosen in the first simple version of dual-action theory.

7.4.2.3. Solution for Second-Order Process. Due to the irregular energy deposition throughout an irradiated medium, one must replace the notion of energy

concentration by the specific energy in a reference sphere. Within the approximation described in the preceding section, one can then assume that the yield E of radiation products from a second-order process will be proportional to the square of the specific energy z:

$$E(z) = cz^2 \tag{7.64}$$

The term *sensitive site* (or *target region*) has occasionally been used. However, this can be misleading. The image of reaction partners moving in an extended region and of sampling with a spherical probe may be more pertinent than that of geometrically defined sites that contain sublesions.

Equation (7.64) applies to one value of the random variable. The observable effect is the average over the distribution of the random variable. As for any random variable, the expectation of the square is equal to the square of the mean of the variable plus its variance [see Eq. (7.54)]:

$$E(D) = c\overline{z^2} = c(\sigma_z^2 + \bar{z}^2) \tag{7.65}$$

The relations for the mean and the variance of the specific energy have been obtained in Section 7.3 [Eqs. (7.53) and (7.61)]:

$$\bar{z} = D \tag{7.66}$$

$$\sigma_z^2 = \zeta D \tag{7.67}$$

where the more usual notion ζ is used, instead of $\bar{z}_d$, for the weighted mean event size:

$$\zeta = \frac{\displaystyle\int_0^\infty z^2 f_1(z)\, dz}{\displaystyle\int_0^\infty z f_1(z)\, dz} = \frac{\overline{z_1^2}}{\bar{z}_f} \tag{7.68}$$

The resulting dose dependence is

$$E(D) = c(\zeta D + D^2) \tag{7.69}$$

This is the main result of the original version of the dual-action model. A purely quadratic dependence on specific energy is transformed into a dose dependence that contains an additional linear term. The linear term is due to the intratrack reactions that occur even at very small doses. The quadratic term is due to the intertrack reactions, which predominate, at least for sparsely ionizing radiations, at larger doses.

The essence of the result is that energy concentrations in the cell or in smaller subcellular sites cannot be arbitrarily low even at very low doses of ionizing radiations. Within the track of charged particles there are always finite energy concentrations. When the dose is sufficiently low, the tracks tend to be separated, and all energy transfers have then in their proximity energy transfers only from the same track. Their statistical frequencies depend on the ionization density within the tracks but not on absorbed dose. The coefficient for the linear term in Eq. (7.69) is the weighted average of the values of specific energy produced in the reference site by individual events, that is, by individual charged particles.

To replace the formal derivation in Section 7.3.4 by an intuitive explanation, one can utilize the diagram of Figure 7.27. In a second-order process a potential reaction partner (an ionization, or a subsequent radiation product) has an efficiency that is proportional to the average number of reaction partners within the sphere of possible interaction. Potential reaction partners can be on the same particle track or on other tracks. The expected number of partners on the same track is proportional to the average event size ζ. This quantity needs to be a weighted average because an energy transfer chosen at random is more likely to be found in those events that contain more ionizations. The average number of reaction partners not on the same track is independent of radiation quality and is merely proportional to absorbed dose. The expected yield is proportional to the product of energy transfers and their expected reaction partners. The first quantity is proportional to absorbed dose, and the second quantity is proportional to the sum of ζ and the absorbed dose:

$$E(D) \propto D(\zeta + D) \tag{7.70}$$

It may appear paradoxical that the average energy density in the vicinity of an energy transfer should be larger than the absorbed dose. Naively one may feel that the contribution of independent tracks had to be reduced to compensate for the presence of the reference track. However, this is a misconception that arises when one disregards the difference between weighted and unweighted sampling. The
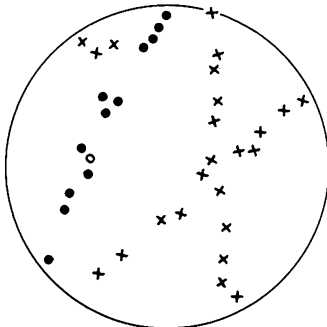
Figure 7.27. Schematic diagram to indicate the intratrack contribution (dots) and the intertrack contribution (crosses) in the same site as a randomly selected transfer (open dot). The contribution of the intratrack term to the specific energy is ζ; the contribution of the intertrack term is D.

point can be explained by the example of a Poisson process of pairs of points. Consider pairs of energy transfers placed with uniform randomness on the plane. For a random point in the plane the circumscribed circle of radius r will contain $kr^2\pi$ dots on the average, where the constant k is the mean number of dots per unit area. This process is called unweighted sampling. One can also perform weighted sampling and select not a random point of the plane but one of the dots (energy transfers). According to the definition of a Poisson process, the presence or absence of other events (pairs of energy transfers) remains uninfluenced by the presence of the selected event. The circle centered at a dot (or a circle positioned randomly over a dot) will always contain the selected dot and, with a probability, p, which depends on the spacing of the dots in a pair and on the radius r of the circle, it will also contain the associated second transfer. Jointly the term $1 + p$ corresponds to the intratrack term ζ. Due to the statistical independence, the expected contribution from other tracks, that is, the analog of the intertrack term, will be $kr^2\pi$. With weighted sampling the average number of transfers contained in a disk is $1 + p + kr^2\pi$.

The analogous argument applies also to a more complicated compound Poisson process. The essential point is that the intratrack term ζ in Eq. (7.70) does not reduce or influence the intertrack term D.

7.4.2.4. Dose–Effect Relation and RBE–Dose Relation.

The linear-quadratic dependence on absorbed dose need not always be the direct result of experimental observations. In cell survival studies, for example, $E(D)$ is not simply the probability for cellular inactivation. Instead, one equates $E(D)$ with the negative logarithm of the survival probability. The resulting relation,

$$S(D) = \exp\left[-E(D)\right] = \exp\left(-aD - bD^2\right) \tag{7.71}$$

is in good agreement with many experimental studies. In other systems the dose dependences are more complicated. For example, in lens opacification studies the severity of effect is measured on an arbitrary numerical scale that is reproducible but provides not more than a ranking of the level of effect. In studies on radiation tumorigenesis similar problems arise, as there are different possibilities to quantify the increase of tumor rates after irradiation. Generally the dose–effect relation need not reflect directly the dose dependence of the underlying cellular damage. However, one can study RBE–dose dependences rather than dose-effect relations. This approach, introduced by Rossi (38), has been applied in many radiobiological studies. It has become an important tool in radiation biophysics for the comparison of the effectiveness of different types of ionizing radiations at specifically low doses.

The RBE of a type of radiation equals the ratio of the dose of a reference radiation (usually γ rays or X rays) to the dose of the specified radiation that produces the same level of effect. In studying RBE one assumes that the observed severity H of the effect, say, for X rays and neutrons, depends on the underlying

and not directly observable cellular damage that is a linear-quadratic function of absorbed dose:

$$H_x(D_x) = H(E(D_x)) = H(\zeta_x D_x + D_x^2)$$

$$H_n(D_n) = H(E(D_n)) = H(\zeta_n D_n + D_n^2) \tag{7.72}$$

Equality of the observed effect implies equality of the arguments in these equations, and one therefore has the relation between the equivalent doses:

$$\zeta_n D_n + D_n^2 = \zeta_x D_x + D_x^2 \tag{7.73}$$

From these equations one obtains the functional dependence of the neutron RBE R_n on neutron dose D_n:

$$R_n = \frac{2(\zeta_n + D_n)}{\zeta_x + [\zeta_x^2 + 4(\zeta_n + D_n) D_n]^{1/2}} \tag{7.74}$$

In the present context it is not necessary to deal with particularities of this dependence (14, 29). An important simplification is, however, the relation that results in the dose range where the underlying dose dependence for densely ionizing radiations is still linear, while it is effectively quadratic for sparsely ionizing radiations. One obtains

$$R_n = \sqrt{\frac{\zeta_n}{D_n}} \tag{7.75}$$

This relation, the inverse proportionality of neutron RBE to the square root of neutron dose, has been a guiding principle in experimental studies not only of cellular but especially of tissue effects, such as radiation tumorigenesis. The investigations have uncovered high values of the RBE of neutrons that agree with the microdosimetric considerations, while they exceed substantially the value 10 of the quality factor utilized for purposes of radiation protection (14). Figure 7.28 represents the RBE–dose dependence according to Eq. (7.74) for the parameters $\zeta_n = 20$ Gy and $\zeta_x = 0$, together with observed relations for lens opacification in the mouse (37) and mammary tumors in the rat (39, 40). (For additional data see Ref. 14.)

In spite of the broad experimental evidence for Eq. (7.75), one cannot exclude the possibility that certain radiation effects have a more complex dependence on specific energy. Although this case may be of less pragmatic importance, it is useful to give the solutions. Utilizing the relations for the moments in Section 7.3.4 and assuming the dependence of the effect probability on specific energy,

$$E(z) = a_1 z + a_2 z^2 + a_3 z^3 \tag{7.76}$$
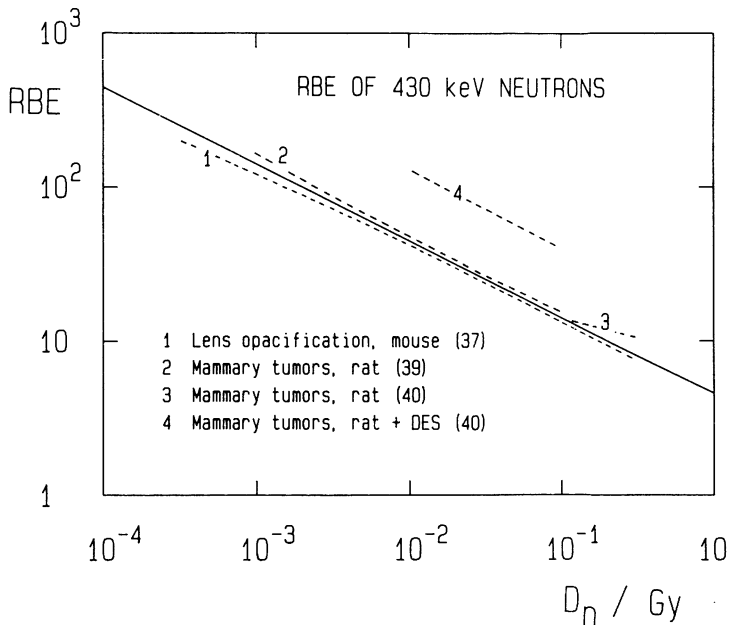
Figure 7.28. Relative biological effectiveness of 430-keV neutrons as a function of neutron dose for lens opacification in mice (37) and for the induction for mammary tumors in Sprague–Dawley (39) and in ACI rats (40). The solid line corresponds to Eq. (7.74) with $\zeta_n = 20$ Gy and $\zeta_i = 0$.

one obtains the dose dependence

$$E(D) = (a_1 + a_2\zeta + a_3\eta)D + (a_2 + 3a_3\zeta)D^2 + a_3D^3$$

where

$$\zeta = \frac{\overline{z_i^2}}{\overline{z_i}} \quad \text{and} \quad \eta = \frac{\overline{z_i^3}}{\overline{z_i}}$$

(7.77)

Higher-order terms could be dealt with similarly. In the considerations of this chapter the general solution will not be required. However, the possible existence of a linear term in specific energy needs to be taken into account in the interpretation of observed linear-quadratic dependences.

7.4.2.5. Site Model and Proximity Model. When an energy transfer or, for simplicity, an ionization happens to be contained in the sampling sphere of diameter d, and if another energy transfer occurs at distance x from it, the latter has a certain probability $U(x)$ to be contained in the same sampling sphere. Here $U(x)$ tends to unity if x is much smaller than d. For larger values of x the function $U(x)$ decreases, and it is zero for x larger than d. The function $U(x)$ is called the geometric reduc-

tion factor; it is an important concept that applies not only to spheres but also to other configurations. The term $U(x)$ is the probability that a random shift in random direction from a random point in the specified object S leads to a point that is still contained in S. For a sphere the solution is

$$U(x) = 1 - \frac{3x}{2d} + \frac{x^3}{2d^3} \qquad 0 \le x \le d \qquad (7.78)$$

This function is given in Figure 7.29. The function $U(x)$ is closely related to the distribution of distances of two random points in the sphere, and this is dealt with in more detail in Section 7.5. The essential point in the present context is that the dual-action model in its simplest form can also be interpreted in terms of a proximity model, that is, a model that applies to a homogeneous site and that postulates not certain critical sites but merely a distance-dependent interaction probability. The simple case of a spherical site corresponds to a distance dependence that is proportional to the function $U(x)$ given in Eq. (7.78) and represented in Figure 7.29. From the standpoint of a proximity model this particular dependence is arbitrary; however, it is not more arbitrary and certainly less unlikely than an assumed threshold dependence (broken line in Figure 7.29). The notion of a threshold dependence was inherent in the treatment by Lea (15), who assumed that biological sublesions (chromosome breaks) can combine if they are formed at a distance closer than a critical value.

There is no reason to assume that either of the two functions in Figure 7.29 equals actual interaction or combination probabilities of sublesions in the cell. The analysis in terms of Lea's proximity model or in terms of the site model is merely an approximation to bring out general characteristics of dose–response relations that may result with different radiation qualities. The simplest proximity model was a convenient choice for the considerations Lea formulated in terms of the LET concept. The site model, on the other hand, is the natural choice for a treatment
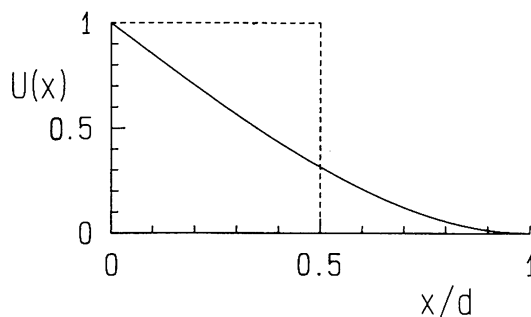

Figure 7.29. Geometric reduction factor $U(x)$ for a sphere of unit diameter. Broken line indicates the distance dependence of the interaction probability invoked in the proximity model of Lea (15).

that utilizes microdosimetric data obtained experimentally with spherical detectors. In spite of their differences, the two models are largely equivalent first approximations. More sophisticated analyses based on different distance dependences are considered in Section 7.5.

7.4.2.6. Limitations of Site Model.

The approximations inherent in the simple form of the dual-action model were noted even in the initial formulation. The most significant simplification is the assumption of a constant interaction probability of energy transfers or sublesions within the assumed site. The assumption is arbitrary. One may, nevertheless, expect that deviations from actual distance dependences should be minor if the compared radiations produce charged particles with ranges exceeding cellular dimensions. Gross inadequacies of the model arise when such radiations are compared to soft X rays, which produce electrons of very short ranges. Nevertheless, even for conventional radiations the comparison of the intratrack and intertrack mechanisms can be biased by the disregard of an increased interaction of energy transfers in close proximity. The reason is that close proximity of transfers within the site is more likely for events on the same track (Figure 7.26). The site model is therefore likely to underestimate the linear intratrack component of the effect.

A further feature of the simple model is the neglect of processes of depletion or competition. The quadratic dependence on specific energy implies the absence of such factors. The simple formulation is valid if there are many potential reaction partners and if only a few of them interact pairwise toward the observed effect. These conditions may largely be fulfilled. For radiation effects such as chromosome aberrations the average lifetime of sublesions, governed by repair, is short enough that only a minor fraction combines. Enzymatic repair processes are highly efficient, at least with sparsely ionizing radiations. Even with densely ionizing radiations a majority of initial lesions is likely to be repaired.

In principle, one can attempt more complex formulations that account for competition of reaction partners. Such approaches would be indicated if one dealt with well-known specific molecular or structural mechanisms. At present the necessary knowledge has not been reached in radiobiology. It is therefore not justified to add minor modifications to the theory, while one retains the crude assumption of spherical sites or of similarly simple geometries, which do not correspond to the reality of the cellular organization.

There is a restriction in the interpretation of the linear component of the dose–effect relation. Deducing a value $\zeta = a/b$ from a linear-quadratic dependence $aD + bD$ and equating it with the weighted mean event size, one disregards a possible component of the effect probability that is inherently linear. The relation

$$E(z) = a_1 z + a_2 z^2 \qquad (7.79)$$

corresponds, in agreement with Eq. (7.77), to the dose dependence

$$E(D) = (a_1 + a_2\zeta)D + a_2D^2 = aD + bD^2 \qquad (7.80)$$

where

$$a = a_1 + a_2\zeta \ , \ b = a_2 \ , \ \frac{a}{b} = \frac{a_1}{a_2} + \zeta$$

The term a/b is therefore merely an upper bound for ζ. Smaller values of ζ corresponding to larger site diameters cannot be excluded. In analogy to considerations in the preceding section, one concludes that any formally derived target size or effective interaction distance is a lower limit. Actual distances will usually be larger.

7.4.2.7. General Considerations on Dual Action. The dual-action model describes a possible mechanism that is consistent with many observed linear-quadratic dose–effect relations and, specifically, with observed dose dependences of RBE of densely ionizing radiations. However, agreement between predicted dose and RBE–dose dependences and radiobiological observations cannot be taken as proof for specific postulates of the model.

The dual-action model is broad. The formalism applies to any second-order process. Such processes can either be due to the combination or accumulation of two lesions or to the combined reaction of two radiation products. The term *interaction* includes reactions of free radicals, energy transport along macromolecules and the resultant production of closely spaced DNA lesions, and the migration and reaction of sublesions, such as chromosome instabilities or breaks. There is as yet no firm evidence which of these mechanisms or which combination of the mechanisms is most relevant. It has also been concluded that the deduced formal interaction distances have only qualitative meaning, and that one deals with interaction or damage accumulation distances that range from nanometers to micrometers (see Section 7.5.4).

Furthermore, the assumed mechanisms and the corresponding equations are of such a general type that they are open to an even wider range of interpretation. In particular, one cannot reject the possibility that one deals not with the pairwise reaction of radiation products or sublesions, but instead with a combined process of highly localized potential lesions and dose-dependent probabilities for repair and/or fixation. Such an interplay of two processes can also have the properties of a second-order reaction.

A dose dependent slowdown or impairment of repair ability has occasionally been invoked as an alternative explanation of the shoulder of the survival curve or other dose–response relations. However, there is little or no evidence for an impairment of enzymatic repair processes at doses of a few grays. Studies, for example by Virsik et al. on chromosome aberrations (41), have established characteristic repair times that are substantially constant up to 10 Gy, that is, up to the highest doses investigated. Similar observations have been obtained in various cell

survival studies. Most of the enzymatic DNA repair processes that are known are of the catalytic type. The enzymes are not used up in the repair process, and under usual conditions it is safe to assume that the concentration of enzymes is sufficient to maintain constant repair efficiency at the concentration of lesions produced by doses of several grays. An exception is the repair enzyme for alkylated DNA bases; it works stoichiometrically, that is, by a suicide reaction. With alkylating agents one obtains a shoulder of the response curve due to the gradual disappearance of the repair enzymes. However, it is doubtful whether similar processes are relevant with ionizing radiations.

Another factor of possible influence on the shoulder of a dose–response curve could be the dose-dependent temporary suppression of DNA synthesis or of cell division. It appears that potentially lethal radiation damage in mammalian cells is partly fixed in an S phase and partly in mitosis. By radiation-induced delay of DNA synthesis or of cell division, a protective effect is achieved, as more time becomes available for repair. If this mechanism were relevant at small and moderate doses but less effective at high doses, it could codetermine the shoulder of the survival curve. Similar effects have been seen, although their role is still uncertain, in studies with Ataxia cells. It has been surmised that the increased sensitivity of these cells to ionizing radiation may not be exclusively due to decreased DNA repair ability, but may also be related to the absence or partial absence of the radiation-induced delay of DNA synthesis.

A detailed analysis would be required to determine the possible influence of such mechanisms, specifically of cell kinetic changes, due to irradiation and any concomitant changes of the proportion of repaired DNA damage. One of the relevant questions in the analysis of such mechanisms is whether the induced delay of DNA synthesis is a dose-dependent process that affects the nucleus of the cell as a whole or whether it is a spatially nonuniform process dependent on the microscopic distribution of energy. There are other potential mechanisms of similar complexity. Present knowledge of the molecular mechanisms is insufficient to verify or reject them. However, any quantitative treatment that may ultimately be reached will have to account for the microdosimetric distributions of energy that determine the biological effectiveness of ionizing radiations.

7.5. PROXIMITY FUNCTION AND ITS APPLICABILITY

7.5.1. Rationale for Distance Model

In the initial formulation of dual radiation action a weak dependence of the interaction probability on distance has been postulated. This assumption has been subsequently been rejected on the basis of two groups of experiments. One group consists, as pointed out in Section 7.4, of studies with low-energy photons, which produce short-range electrons with energies between a few hundred electronvolts to several kilo-electronvolts (30, 31). These particles are substantially more efficient than Eq. (7.69) would predict with the parameter ζ for site sizes near 1 μm.

One concludes that energy transfers in close proximity are particularly effective. In other words, the interaction probabilities over small distances are substantially larger than those for larger distances. Interaction over larger distances, with greatly reduced probability, must nevertheless be assumed to explain the curvature of dose-response relations obtained with sparsely ionizing radiations.

A combination of pairs of reactants or of sublesions would not need to be postulated if one could invoke other factors (such as the ones mentioned in Section 7.4.2) to explain the curvature of the dose relation. But the latter processes would also be inherently quadratic, and the interplay of the two modes of damage would have to be quantified in terms of spatial and temporal interrelations.

The second group of experiments, namely the investigations of Rossi et al. (32–34), with spatially correlated heavy ions also showed that the interaction probabilities are greatly increased for energy transfers in close proximity, that is, at distances less than 100 nm. On the other hand, one found, both for cell killing and for chromosome aberrations, that the correlated protons, although separated by distances on the order of 100 nm, were more efficient than the same particles with no spatial correlation (see Figure 7.25). In this way the experiments have not only demonstrated the increase of the interaction probability with increasing spatial proximity of energy transfers but they have also shown the presence of a small interaction probability extending to larger distances. This latter finding is in line with the conclusions drawn earlier (6, 12, 15) from the curvature in dose–effect relations for cell survival or for the production of chromosome aberrations. But the experimental evidence is somewhat more specific. It proves that the effect is not merely a gross dose-dependent process (for example, reduction of repair) but is also a result of the spatial proximity of two charged particle tracks.

The evidence from the soft X ray experiments and the correlated ion studies has motivated a further development of the model of dual radiation action and a formal treatment that takes into account a distance-dependent interaction probability between energy transfers or sublesions (42). A precondition for the modified treatment was the earlier development of new microdosimetric concepts that are more closely linked to the computational approach than to microdosimetric measurements (44, 45). The biophysical considerations are related to the problem of the random intercept of geometric objects. Essential results are, therefore, introduced first in purely geometric terms. They can then be applied readily to the energy deposition problem.

Energy deposition in a cellular structure by a charged particle is a stochastic process that can be seen as the random intersection of two geometric objects, the site S and the particle track T. The site is assumed to be part of a uniform medium and, furthermore, the radiation field is taken to be uniform. A particle track is the random configuration of energy transfers produced by a charged particle and/or its secondaries. Figure 7.30 gives a diagram that explains the notion of energy transfers ϵ, that is, the individual energy deposits, which may either be ionizations or excitations. The term *particle track* denotes the set of all transfers produced by a charged particle and its secondaries. Each transfer point is ascribed a value of
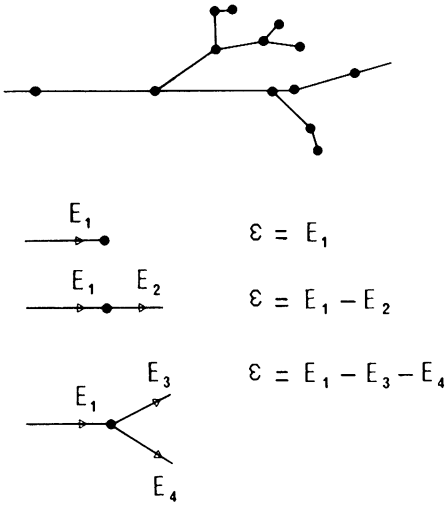
$$\varepsilon = E_1$$

$$\varepsilon = E_1 - E_2$$

$$\varepsilon = E_1 - E_3 - E_4$$

Figure 7.30. Schematic diagram of a segment of a charged particle track with indication ($\bullet$) of the transfer points and the corresponding energy transfers ϵ.

energy that equals the energy of the incident ionizing particle minus the energy of the emerging ionizing particle(s). These notions are utilized in Section 7.5.3. For the present geometric considerations it is sufficient to note that the site is a certain domain and that the track is also a geometric object. Frequently, as in the preceding sections, a simple geometry is postulated for the site. However, the subsequent considerations apply generally to domains that may be of complicated shape and need not be simply connected. The particle tracks are subdimensional structures, that is, sets of points. Nevertheless, one could visualize each transfer point as a small sphere with volume proportional to the corresponding energy transfer. Thus, a simple analogy between energy and volume is established, and the geometric theorems can readily be applied to the biophysical problem of the interception of cellular structures by charged particle tracks.

7.5.2. Mean and Weighted Mean of Random Overlap of Geometric Objects

7.5.2.1. Random Intercept of Two Domains. Assume that two geometric objects S and T are randomly superimposed in the sense of isotropic, uniform randomness. This type of randomness, also termed μ randomness, corresponds to the situation where one of the objects is in a fixed position while the other object has a uniformly and isotropically distributed random position. A different concept termed weighted randomness, or ν randomness, will also be considered. The two types of randomness were originally introduced in the context of random processes of straight lines (43). A more general use of the concepts in microdosimetric calculations (44, 45) led to a definition for arbitrary geometries (46).

Figure 7.31 illustrates the two types of randomness. Here S is represented by a circular site and T by linear tracks of variable size to indicate the general case. For
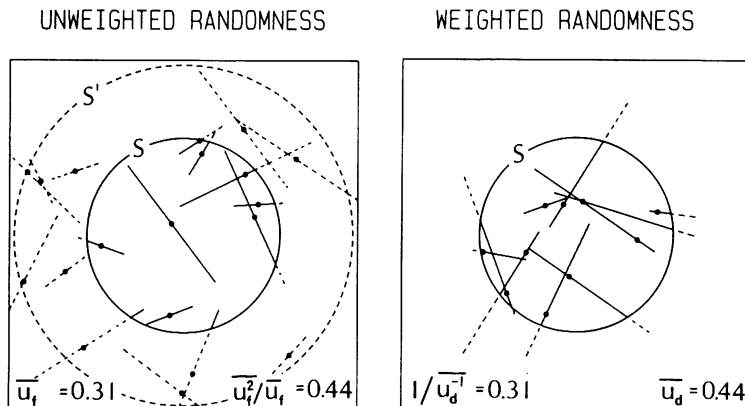
UNWEIGHTED RANDOMNESS   WEIGHTED RANDOMNESS

Figure 7.31. Linear tracks of length 0.25 and 0.75 intercepting a unit diameter circular site S. The intercepts with S are drawn as solid line segments. The dots are the random points that determine the position of the tracks according to the definition of the two types of randomness (see text). The mean intercept, 0.31, and the weighted mean intercept, 0.44, result with the two types of sampling as indicated in the diagrams.

μ randomness the object T is assumed to have a reference point C taken to be the center in the tracks of Figure 7.31 (left panel). Consider a region S' that contains S and all potential positions of C that permit an overlap between S and T. A random point R uniformly distributed in S' is chosen, and T—or, in the general case, an element of the set of objects T—is positioned with random orientation so that its reference point C coincides with R. Repeating this procedure and disregarding all events with no intercept of S and T, one obtains a probability distribution $f(u)$ of size u of the intercepts $U = T \cap S$. In the example of Figure 7.31 (left panel) there are 10 intercepts.

Weighted randomness (ν randomness) is obtained as follows. Two independent random points P_S and P_T are selected that are distributed uniformly and independently in S and T. If there is a set of objects T, each element has a selection probability proportional to its measure. The relative frequency of the larger objects is therefore enhanced in weighted sampling. Although short and long tracks are taken to be equally frequent in the example, there are far more long tracks in the right panel of Figure 7.31, which corresponds to weighted sampling. The selected object T is positioned with random orientation so that the points P_S and P_T coincide. With this procedure [originally introduced for sampling procedures in microdosimetric computations (44)] there is always a positive intercept u. In an extension of the earlier result of Kingman (43) for straight lines, it has been shown (46) that the distribution $d(u)$ of intercepts under weighted randomness is related to the distribution of intercepts for uniform, isotropic randomness:

$$d(u) = \frac{u\,f(u)}{\displaystyle\int_0^{u_{max}} u\,f(u)\,du} = \frac{u\,f(u)}{\bar{u}_f} \qquad (7.81)$$

The relation holds for arbitrary shapes of the geometric objects S and T. Weighted sampling can therefore be used as an efficient procedure to obtain not only the distribution $d(u)$ but also the distribution $f(u)$ and its moments. In Figure 7.31 two important identities are indicated for the unweighted and the weighted mean intercept:

$$\bar{u}_f = \frac{1}{\overline{u_d^{-1}}} \quad \text{and} \quad \frac{\overline{u_f^2}}{\bar{u}_f} = \bar{u}_d \tag{7.82}$$

The weighted average $\bar{u}_d$ is always larger than the unweighted average $\bar{u}_f$. The difference determines the variance of the intercept under μ randomness:

$$\sigma^2 = \overline{u_f^2} - \bar{u}_f^2 = (\bar{u}_d - \bar{u}_f)\bar{u}_f \tag{7.83}$$

Blaschke (47) and Santalo (48) have derived an equation, the fundamental kinematic formula, which determines, among other quantities, the mean intercept $\bar{u}_f$:

$$\bar{u}_f = \frac{V_S V_T}{A} \tag{7.84}$$

where V_S is the volume of S and V_T the measure of T, while A is the volume of the Minkowski product [also called dilatation (49)] of S and T. In the present case, where isotropic randomness is considered, the volume of the Minkowski product is averaged over all directions (for an elementary treatment of these matters see Ref. 50). If S is a spherical region, A is equal to the associated volume of T, one of the important notions introduced by Lea (15) to radiation biophysics.

A further result is of great generality and of special importance in the context of the present chapter. This is the relation for the mean overlap $\bar{u}_d$ of S and T under weighted randomness (46):

$$\bar{u}_d = \int_0^{x_{max}} \frac{t(x)\, s(x)}{4\pi x^2}\, dx \tag{7.85}$$

where x_{max} is the maximum point pair distance in S or T, whichever is smaller. The two functions $s(x)$ and $t(x)$ are called proximity functions of S and T; they could also be called spatial autocorrelation functions. The proximity functions are equal to the probability distributions of distances between pairs of independent random points in the objects multiplied by the volume of the objects. Thus, $s(x)$ dx/V is the probability that two random points in S are separated by a distance between x and $x + dx$. If a geometric object is a random configuration, its proximity function is the volume-weighted average of the proximity functions for all possible configurations.

Equation (7.85) is the reason that the proximity functions are important characteristics of geometric objects. The functions have been derived for simple ge-

ometries such as spheres, spheroids, spherical shells, cylinders, cubes, or slabs (e.g., Ref. 43). For more complicated geometries such as charged particle tracks Monte Carlo computations may be required (Section 7.5.3).

If a domain is not subdimensional, it is often convenient to utilize a related quantity, the geometric reduction factor, a concept introduced originally by Berger (51) in the context of dosimetric computations:

$$U(x) = \frac{s(x)}{4\pi x^2} \qquad (7.86)$$

As stated in Section 7.4, $U(x)$ is equal to the probability that a random point in S remains in S after it is shifted by the distance x in a random direction.

7.5.2.2. Intercept of Site by Poisson Process of Geometric Objects.

In many applications one deals with the intercept of a domain S by a Poisson process of geometric objects, T. The Poisson process, also called a Boolean scheme (52), results from a uniform, isotropic field of objects, T, with a density of λ objects per unit volume. Nominal coverage is $\psi = V\lambda$, where V is the mean volume of T. One will realize in Section 7.5.4 that ψ is the analog of absorbed dose D.

The volume u of the intercept of the Poisson process with S can be defined either as the sum of the volumes of all intercepts or as the volume of the union of all intercepts. The former case is considered first and is referred to in the subsequent sections. It corresponds to a compound Poisson process. The expected intercept is

$$\bar{u}(\psi) = V_S \psi \qquad (7.87)$$

and with Eq. (7.53) for the compound Poisson process one obtains the second moment:

$$\overline{u^2}(\psi) = [\bar{u}_d + \bar{u}(\psi)]\bar{u}(\psi) = (\bar{u}_d + V_S\psi)V_S\psi \qquad (7.88)$$

This is the geometric analog of the basic result for dual radiation action.

A more complicated result is obtained (46) when u is the measure of the union of all intercepts, that is, when multiple overlap is not weighted with the corresponding multiplicity:

$$\bar{u}(\psi) = V_S[1 - \exp(-\psi)]$$
$$\overline{u^2}(\psi) = [u^* + \bar{u}(\psi)]\bar{u}(\psi) \qquad (7.89)$$

where

$$u^* = \frac{\int_0^{x_{max}} s(x)[\exp(\psi t(x)/4\pi x^2) - 1]\, dx}{\exp(2\psi) - \exp(\psi)}$$

Although this result is related to possible formulations of the saturation problem in cellular radiation action, too little is yet known about actual mechanisms to make quantitative formulations worthwhile. The result is here cited in view of its generality and the potential applications to a broad range of problems of stochastic geometry. It is also given to elucidate the point that, in the presence of saturation, a second-order process with nonhomogeneous kinetics need not lead to a linear-quadratic dependence on dose.

7.5.3. Application to Energy Deposition Problem

7.5.3.1. Proximity Function of Energy Transfers. The results of the preceding section can be applied to the energy deposition problem to obtain a generalized formulation of dual radiation action. Furthermore, apart from any particular application, the proximity function for a radiation field affords a fundamental characterization of radiation quality that extends the LET concept and links it to the conventional microdosimetric quantities.

The concept of the proximity function $t(x)$ of particle tracks is analogous to that of the geometric proximity function, with the modification that energy replaces volume. In analogy to the volume proximity function, the energy proximity function $t(x)$ can be understood as the distribution of pair distances of energy transfers multiplied by the total energy of the track. The proximity function includes a delta function at $x = 0$ that is proportional to the weighted mean of individual energy transfers ϵ_i. More formal definitions have been given elsewhere (14, 20, 45).

The actual computation is best explained in terms of the integral proximity function

$$T(x) = \int_0^x t(s) \, ds \tag{7.90}$$

From a simulated track $T(x)$ is obtained by considering all pairs of transfer points that are separated by a distance less than x:

$$T(x) = \frac{\sum_{i,k} \epsilon_i \epsilon_k}{\sum_i \epsilon_i} \tag{7.91}$$

where the summation runs over all i and over all transfer points k separated by distance up to x from the transfer point i. The value $T(0)$ determines the delta function $T(0) \, \delta(x)$ in $t(x)$. It results from the pairs with $i = k$:

$$T(0) = \frac{\sum \epsilon_i^2}{\sum \epsilon_i} \tag{7.92}$$

Equation (7.91) implies that $T(x)$ equals the expected energy on the particle track in a sphere centered on a randomly selected energy transfer. Accordingly, $t(x) \, dx$ is the expected energy within the distance interval x to $x + dx$ from a randomly selected energy transfer.

One can also consider the proximity function that contains the trivial dose-dependent intertrack term from unrelated particles:

$$t(x; D) = t(x) + 4\pi x^2 \rho D \tag{7.93}$$

With the density $\rho = 1$ g/cm^3 and with the units electronvolts, nanometers, and grays one obtains the following relation, which permits a convenient comparison of the relative magnitude of the intratrack and intertrack contributions:

$$t(x; D) = t(x) + 7.82 \times 10^{-5} \, x^2 D \tag{7.94}$$

In computations the proximity function is derived by sampling all pairs of energy transfers in a sufficiently large number of simulated particle tracks. If the particle tracks have different initial energies, the proximity function is the energy-weighted average for the different tracks. Proximity functions have been computed for electrons and for track segments of heavy ions (44, 53–56). Figure 7.32 represents the differential proximity function $t(x)$ for electrons of energy up to 10 keV. The upper panel contains also the dose-dependent intertrack term for doses of 10 and 100 Gy. The comparison shows clearly that damage accumulation over short distances is entirely determined by the intratrack term even at high doses.

In the simplest LET approximation one pictures the tracks as straight lines with an average value of LET, which ought to be not the track average $\bar{L}_f$ but the dose average $\bar{L}_d$. The proximity function is then a constant:

$$t(x) = 2\bar{L}_d \tag{7.95}$$

This is not a good approximation. The approximation in terms of linear tracks with LET varying according to the continuous slowing-down (CSD) approximation is also of limited applicability, as shown in Figure 7.33. At small distances the LET approximation indicates energy concentrations that are too low because no account is taken of energy loss straggling, that is, the discontinuous structure of the electron tracks. The fluctuations of energy loss must therefore be taken into account if the LET concept is to be applied to electrons. On the other hand, one sees from the figures that the correlated energy transfers at larger distances are overestimated with the LET concept and linear tracks. This is due to the neglect of angular scattering, which leads to curled electron tracks. However, one obtains a fairly good approximation to the proximity functions when one depicts the electron tracks as linear segments with continuous, constant energy loss and two-thirds of their CSD range.

For track segments of heavy ions the influence of straggling and radial energy distribution can be separated (44, 45). The proximity function is then the sum of
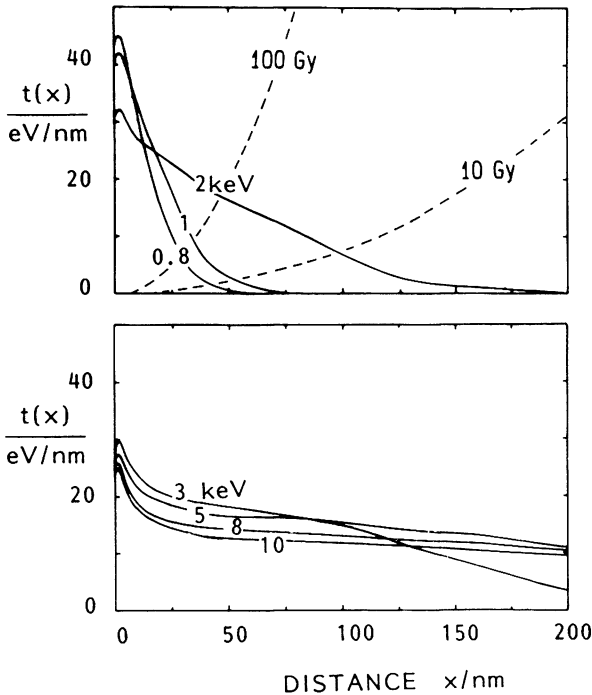
Figure 7.32. Proximity functions $t(x)$ for low-energy electrons (from Ref. 53). Broken lines in the upper panel give the contribution due to unrelated tracks, that is, the intertrack contribution, at doses of 10 and 100 Gy.

a term $t_\delta(x)$, which is the weighted average of the proximity functions for all δ rays, and a term that is equal to the proximity function of a continuous track with the same radial energy distribution as the actual track:

$$t(x) = t_\delta(x) + Lt_a(x) \qquad (7.96)$$

where $t_a(x)$ refers to an amorphous track that averages out the structure of the δ rays. The term contains the stopping power L as a factor; $t_a(x)$ depends only on the radial distribution of dose and can be calculated from it. Figure 7.34 gives integral proximity functions for track segments of heavy ions with an energy of 20 MeV/nucleon and indicates their separation into the term $t_\delta(x)$ and the term for the continuous track. Where the δ term (dotted line) is a minor part of $T(x)$, the random occurrence of the δ rays can be disregarded, although the lateral energy transport by δ rays may still be an important factor.

The graphs of the differential proximity function in Figure 7.32 can be understood rather directly. Here $t(x)$ is a spatial autocorrelation function of the charged particle tracks, that is, it gives the distribution in distance of the potential reaction partners around a randomly chosen energy transfer. Distance distributions for sub-
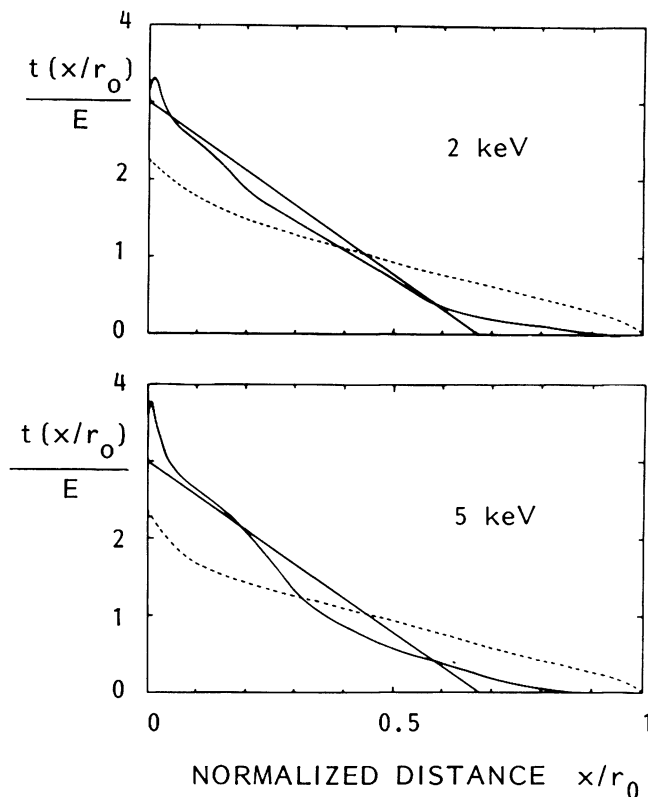
Figure 7.33. Comparison of proximity functions for electrons (solid curves) with functions that result from simplified models (from Ref. 53). The dashed curves are obtained if the electron tracks are treated as straight lines with LET from the CSD approximation. The solid straight lines result if the tracks are pictured as straight lines with constant energy loss rate and ranges equal to two-thirds of the CSD range. The ranges and LET values are for water. The curves show that the LET approximation fails to account for energy loss straggling and angular scattering.

sequent radiation products, such as free radicals, are modified due to diffusion or energy transport processes. An example for proximity functions subjected to diffusion is given in Figure 7.35. Zaider and Brenner (57) have applied proximity functions and distance distributions to radiation chemistry. Such applications may be expected to play an increasing role in problems of nonhomogeneous kinetics.

7.5.3.2. Relation between Proximity Function and Weighted Mean Event Size.
Equation (7.85) implies one of the central theorems of microdosimetry. The weighted average of energy imparted per event to a site S is

$$\bar{\epsilon}_d = \int_0^{x_{max}} \frac{t(x)s(x)}{4\pi x^2} \, dx = \int_0^{x_{max}} t(x)U(x) \, dx \tag{7.97}$$
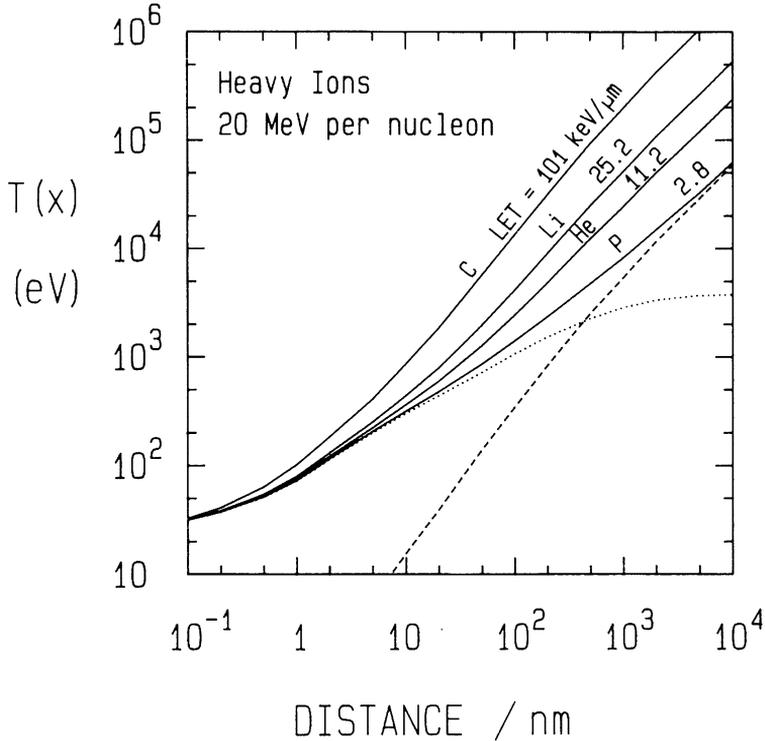
Figure 7.34. Integral proximity functions $T(x)$ for different heavy ions of kinetic energy 20 MeV/ nucleon (from Ref. 44). The dotted line represents the contribution, $T_\delta(x)$, due to δ rays. The dashed line corresponds to the LET-dependent term for protons. For the heavier ions this latter term is multiplied by a factor corresponding to the increased LET [see Eq. (7.96)].

where $t(x)$ is the proximity function of the radiation, and $s(x)$ and $U(x)$ are the proximity function and the geometric reduction factor of the site. For the sphere of diameter d one obtains, with Equation (7.78), the important equation

$$\bar{\epsilon}_d = \int_0^d \left(1 - \frac{3x}{2d} + \frac{x^3}{2d^3} \right) t(x) \, dx \qquad (7.98)$$

The weighted mean linear energy and mean specific energy per event are obtained from the relations

$$\bar{y}_d = \frac{\bar{\epsilon}_d}{\bar{l}} \quad \text{and} \quad \zeta = \frac{\bar{\epsilon}_d}{m} \qquad (7.99)$$

where the mean chord length $\bar{l}$ equals $4V/S$ for a convex site of volume V and surface area S, and m is the mass of the site.
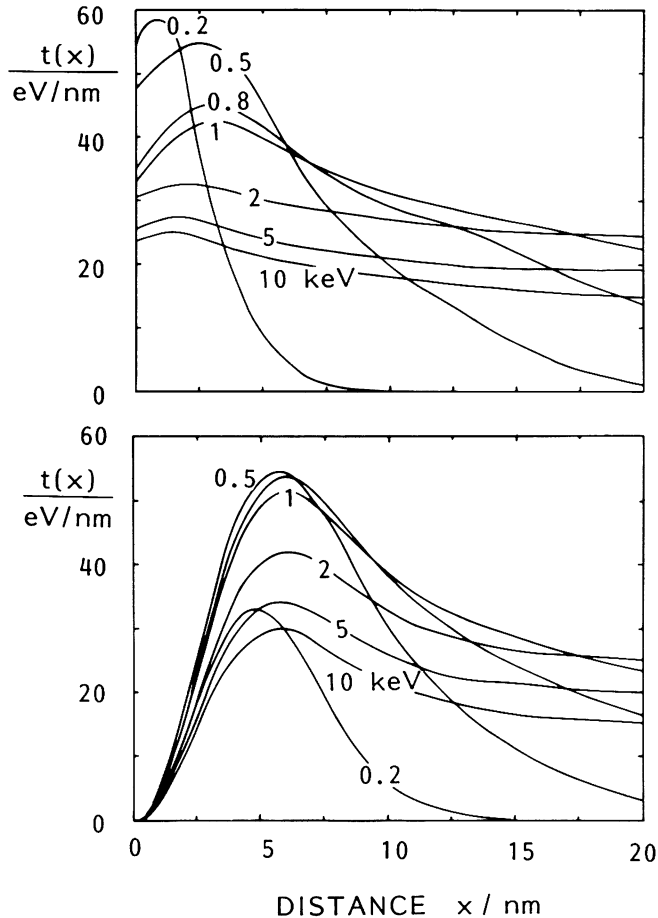
Figure 7.35. Initial parts of the proximity functions for electrons in water and the functions that result if the inchoate pattern of energy transfers has diffused by a characteristic distance of 5 nm. The characteristic distance is the mean separation that results due to the diffusion for two points initially coinciding (from Ref. 53).

Equation (7.97) permits the derivation of the weighted mean event size and therefore also of the variance ζD of the specific energy in any structure, even one of complex shape. This gives broad applicability to Eq. (7.69), that is, to the result for the site model of dual radiation action. In Section 7.5.4 it will be shown that Eq. (7.97) can also be modified to account for a distance model.

The function $t(x)$ cannot be measured directly with present experimental methods, but it can, at least in principle, be derived from measured values of $\bar{y}_d$, ζ, or $\bar{\epsilon}_d$ (58). It can be computed readily from simulated charged particle tracks. The use of the proximity function obviates the need to measure the quantities $\bar{y}_d$ or ζ for different geometries. If the function $t(x)$ for a radiation is known, one merely

needs the geometric proximity function $s(x)$ for the site to compute the microdosimetric parameters. The geometric proximity function can be expressed analytically for simple geometries. In other cases it can be obtained from Monte Carlo simulations. Although one may not often find it necessary to compute microdosimetric parameters for irregular geometries, the use of Eq. (7.97) can be essential in general considerations. Even complicated sites can have fairly simple proximity functions. For example, small targets uniformly distributed over a spherical region have, except for small distances comparable to the targets, a proximity function equal to that of the sphere. Accordingly, one expects, even for the complicated structure, the linear-quadratic relation of Eq. (7.69) with the parameter ζ for the spherical site. The general relation is also important because it implies that microdosimetric parameters for spherical and cylindrical regions can be nearly equal (59). This reduces substantially the need for complicated detectors, particularly in charged particle fields where wall-less microdosimetric instruments are required (60).

In the context of models of cellular radiation action proximity functions can be employed to account more rigorously for spatial correlations of energy transfers and subsequent sublesions than did the simple site model or the earlier distance model of Lea.

7.5.4. General Formulation of Dual Radiation Action

In the following brief treatment *interaction of pairs of energy transfers* is again used as a convenient shorthand expression. It refers to a mechanism whereby sublesions are formed by two energy transfers and where they interact to form a lesion. The sublesions could be molecular alterations in DNA, for example, single-strand breaks in close proximity; the "interaction" would then be misrepair due to the interference of excision repair of the two single-strand breaks. The sublesions could also be alterations on a more complex level, for example, pairs of double-strand breaks in chromosomal structures that may form chromosome aberrations by misrepair.

The probability of an energy transfer to be transformed into a lesion is assumed to be proportional to the sum of its neighboring transfers, the contribution of each transfer being weighted by a distance-dependent interaction probability $\gamma(x)$. Accordingly, one obtains the probability of interaction of an energy transfer ϵ_i:

$$P_i = \epsilon_i \int_0^\infty t(x; D) \, \gamma(x) \, dx \tag{7.100}$$

where $t(x; D)$ is the proximity function that includes the trivial dose-dependent term due to independent particle tracks [Eq. (7.93)]. To simplify the resulting formulas, it is practical to normalize $\gamma(x)$ so that its spatial integral is unity:

$$\int_0^\infty \gamma(x) 4\pi x^2 \rho \, dx = 1 \tag{7.101}$$

The interaction probability is therefore

$$P_i = k\epsilon_i \left[\int_0^\infty t(x)\gamma(x) \, dx + D \right] \tag{7.102}$$

The total yield, $E(D)$, of lesions, arbitrarily normalized to unit mass, is then

$$E(D) = kD \left[\int_0^\infty t(x)\gamma(x) \, dx + D \right] = k(\xi D + D^2) \tag{7.103}$$

The main result is that one obtains, as in the simple site model, a linear-quadratic dose dependence. The coefficient ξ of the linear term is, as with the site concept, a measure of an effective local concentration of energy transfers in the individual charged particle tracks of the radiation. One can consider the result for the site model [that is, Eq. (7.69)] as a special case of the present formula. If one assumes that an energy transfer has constant interaction probability with all transfers within the same site and zero interaction probability with transfers outside the site, the function $\gamma(x)$ will be equal to the geometric reduction factor $U(x)$ divided by m. The dose dependence is then

$$E(D) = kD \left[\frac{\displaystyle\int_0^\infty t(x)U(x) \, dx}{m} + D \right] = k(\zeta D + D^2) \tag{7.104}$$

This is the earlier result for the site model.

In actuality, the site and proximity aspects play joint roles. The function $\gamma(x)$ is the product of two terms representing the inherent dependence on distance and the influence of the geometry of the site, $\gamma(x) = g(x)U(x)$. Usually it will be difficult in an experiment to separate the two factors. The aim of the biophysical investigations of cellular radiation action is to determine the compound function $\gamma(x)$.

These considerations describe the general approach, but additional factors play a role. There may be, as pointed out in Section 7.4.2, an inherently linear component in the dependence of the effect on z. Furthermore, the quadratic term in absorbed dose is, unlike the linear intratrack term, dependent on dose rate. In spite of such added complexities, the formulation in terms of the proximity function has led to definite conclusions when applied to experiments with correlated heavy particles or to the experiments with soft X rays (30–34). It is found that $\gamma(x)$ decreases sharply at small distances but reaches out to distances on the order of several micrometers (33, 34). Due to the abundance of neighboring energy transfers in close proximity, the linear term results mostly from short-range interactions. Due to the relatively large number of more distant energy transfers from independent tracks, the quadratic component results largely from the interplay of radiation

products formed in independent particle tracks. This difference and the influence of the time factor on the quadratic component account for a different effect of various dose-modifying factors on the linear and the quadratic component in dose dependences of cellular radiation effects.

Models of cellular radiation action are still tentative. More needs to be known about the molecular mechanisms, but it follows from the different effectiveness of sparsely and densely ionizing radiations that the mechanisms are greatly affected by the spatial correlation of energy in cellular and subcellular structures. Microdosimetric concepts and data will, therefore, remain essential in any stochastic model of the effects of radiation on cells.

REFERENCES

1. B. Alberts, D. Bray, J. Lewis, M. Raff, K. Roberts, and J. D. Watson, *Molecular Biology of the Cell*, Garland, New York and London, 1983, Chapter 1, p. 4.

2. N. V. Timofeeff-Ressowsky and K. G. Zimmer, *Das Trefferprinzip in der Biologie*, Hirzel, Leipzig, 1947.

3. G. Hotz, *Z. Naturforschg.* **21b**, 148–152 (1966).

4. F. Dessauer, *Z. Physik* **84**, 218 (1933).

5. K. G. Zimmer, *Studies on Quantitative Radiation Biology*, Oliver and Boyd, London, 1961.

6. O. Hug and A. M. Kellerer, *Stochastik der Strahlenwirkung*, Springer-Verlag, Berlin, 1966.

7. F. Dessauer, *Z. Physik* **12**, 38–47 (1923).

8. J. A. Crowther, *Proc. Roy. Soc. (London)* **B96**, 207 (1924).

9. P. Jordan, *Naturwissenschaften* **26**, 537 (1938).

10. C. Lücke-Huhle, W. Comper, L. Hieber, and M. Pech, *Radiat. Environ. Biophys.* **20**, 171 (1982).

11. H. H. Rossi, *Radiat. Environ. Biophys.* **20**, 1 (1981).

12. A. M. Kellerer and O. Hug, *Biophysik* **1**, 33 (1963).

13. *Quantitative Concepts and Dosimetry in Radiobiology*, ICRU Report 30, International Commission on Radiation Units and Measurements, Washington, DC, 1979.

14. A. M. Kellerer and H. H. Rossi, in *Cancer, A Comprehensive Treatise*, Vol. 1, 2nd. ed., F. F. Becker (Ed.), Plenum, New York, 1982, pp. 569–616.

15. D. E. Lea, *Actions of Radiations on Living Cells*, 2nd ed., Cambridge University Press, London, 1955.

16. H. H. Rossi, *Radiat. Res.* **10**, 522 (1959).

17. H. H. Rossi, *Radiat. Res.* Suppl. 2, 290 (1960).

18. H. H. Rossi, in *Advances in Biological and Medical Physics*, Vol. 11, J. H. Lawrence and J. W. Gofman (Eds.), Academic, New York, 1967, pp. 27–85.

19. H. H. Rossi, *Radiation Dosimetry*, Vol. 1, *Fundamentals*, F. H. Attix and W. C. Roesch (Eds.), Academic, New York, 1968, pp. 43–92.

20. *Microdosimetry*, ICRU Report 36, International Commisssion on Radiation Units and Measurements, Bethesda, MD, 1983.

21. *Radiation Quantities and Units*, ICRU Report 33, International Commission on Radiation Units and Measurements, Washington, DC, 1980.

22. M. G. Kendall and P. A. P. Moran, *Geometrical Probability*, Griffin, London, 1963.

23. A. M. Kellerer, *Radiat. Res.* **98,** 425 (1984).

24. A. M. Kellerer, *Mikrodosimetrie, Grundlagen einer Theorie der Strahlenqualität*, Series of Monographs B1, Gesellschaft für Strahlenforschung, Munich, 1968, pp. 1–157.

25. A. M. Kellerer, in *Proceedings of the 2nd Symposium on Microdosimetry*, Euratom 4452 d-f-e, H. G. Ebert (Ed.), Brussels, 1970, pp. 107–134.

26. A. M. Kellerer, in *Techniques in Radiation Dosimetry*, K. R. Kase and B. E. Bjärngard (Eds.), Academic, in press.

27. J. Booz and M. Coppola, *Proceedings of the 4th Symposium on Microdosimetry*, Vol. II, J. Booz et al. (Eds.), Euratom 5122 d-e-f, Luxembourg, 1974, pp. 983–998.

28. H. H. Rossi, M. H. Biavati, and W. Gross, *Radiat. Res.* **15,** 431 (1961).

29. A. M. Kellerer and H. H. Rossi, *Curr. Top. Radiat. Res. Quarterly* **8,** 85 (1972).

30. D. T. Goodhead and D. J. Brenner, *Proceedings of the 8th Symposium on Microdosimetry*, J. Booz and H. G. Ebert (Eds.), Euratom 8395, Luxembourg, 1983, pp. 597–609.

31. R. P. Virsik, D. T. Goodhead, R. Cox, J. Thacker, Ch. Schäfer, and D. Harder, *Int. J. Radiat. Biol.* **38,** 545 (1980).

32. H. H. Rossi, *Radiat. Res.* **78,** 185 (1979).

33. A. M. Kellerer, Y.-M. P. Lam, and H. H. Rossi, *Radiat. Res.* **83,** 511 (1980).

34. M. Zaider and D. J. Brenner, *Radiat. Res.* **100,** 213 (1984).

35. G. R. Merriam, Jr., B. J. Biavati, J. L. Bateman, H. H. Rossi, V. P. Bond, L. Goodman, and E. F. Focht, *Radiat. Res.* **25,** 123 (1965).

36. H. H. Smith and H. H. Rossi, *Radiat. Res.* **28,** 302 (1966).

37. J. L. Bateman, H. H. Rossi, A. M. Kellerer, C. V. Robinson, and V. P. Bond, *Radiat. Res.* **51,** 381 (1972).

38. H. H. Rossi, *Phys. Med. Biol.* **15,** 255 (1970).

39. C. J. Shellabarger, D. Chmelevsky, and A. M. Kellerer, *J. Nat. Cancer Inst.* **64,** 821 (1980).

40. C. J. Shellabarger, D. Chmelevsky, A. M. Kellerer, and J. P. Stone, *J. Nat. Cancer Inst.* **69,** 1135 (1982).

41. R. P. Virsik, R. Blohm, K.-P. Herman, H. Modler, and D. Harder, *Proceedings of the 8th Symposium on Microdosimetry*, J. Booz and H. G. Ebert (Eds.), Euratom 8395, Luxembourg, 1982, pp. 409–422.

42. A. M. Kellerer and H. H. Rossi, *Radiat. Res.* **75,** 471 (1978).

43. J. F. C. Kingman, *J. Appl. Prob.* **2,** 162 (1965).

44. D. Chmelevsky, *Distributions et Moyennes des Grandeurs Microdosimetriques a l'echelle du Nanometre*, Rapport CEA-R-4785, Service de Documentation, C. E. N. Saclay. B.P.2—F-91190 Gif s. Yvette, 1976.

45. A. M. Kellerer and D. Chmelevsky, *Radiat. Environ. Biophys.* **12,** 321 (1975).

46. A. M. Kellerer, *J. Appl. Prob.* **23,** 307 (1986).

47. W. Blaschke, *Math. Z.* **42**, 399 (1937).

48. L. A. Santalo, *Integral Geometry and Geometric Probability*, Addison-Wesley, London, 1976.

49. J. Serra, *Image Analysis and Mathematical Morphology*, Academic, London, 1982.

50. A. M. Kellerer, *Proceedings of the 7th Symposium on Microdosimetry*, Vol. II, J. Booz, H. G. Ebert, and H. D. Hartfiel (Eds.), Euratom 7147 DE-EN-FR, Harwood Academic Publishers, London and New York, 1981, pp. 1049–1062.

51. M. J. Berger, in *Medical Radionuclides: Radiation Dose and Effects*, R. J. Cloutier, C. L. Edwards, and W. S. Snyder (Eds.), USAEC Report CONF-691212, National Technical Information Service, Springfield, VA, 1970, pp. 63–86.

52. G. Matheron, *Random Sets and Integral Geometry*, Wiley, New York, London, Sydney, and Toronto, 1974.

53. D. Chmelevsky, A. M. Kellerer, M. Terrissol, and J. P. Patau, *Radiat. Res.* **84**, 219 (1974).

54. H. G. Paretzke and F. Schindel, *Proceedings of the 7th Symposium on Microdosimetry*, Vol. I, J. Booz, H. G. Ebert, and H. D. Hartfiel (Eds.), Euratom 7147 DE-EN-FR, Harwood Academic Publishers, London and New York, 1981, pp. 387–398.

55. B. Grosswendt, *Proceedings of the 7th Symposium on Microdosimetry*, Vol. I, J. Booz, H. G. Ebert, and H. D. Hartfiel (Eds.), Euratom 7147 DE-EN-FR, Harwood Academic Publishers, London and New York, 1981, pp. 319–328.

56. F. Zilker, U. Mäder, and H. Friede, *Proceedings of the 7th Symposium on Microdosimetry*, Vol. I, J. Booz, H. G. Ebert, and H. D. Hartfiel (Eds.), Euratom 7147 DE-EN-FR, Harwood Academic Publishers, London and New York, 1981, pp. 449–456.

57. M. Zaider and D. J. Brenner, *Radiat. Res.* **100**, 245 (1984).

58. M. Zaider, D. J. Brenner, K. Hanson, and G. N. Minerbo, *Radiat. Res.* **91**, 95 (1982).

59. A. M. Kellerer, *Radiat. Res.* **86**, 277 (1981).

60. W. A. Glass and W. A. Gross, in *Topics in Radiation Dosimetry, Supplement 1*, F. H. Attix (Ed.), Academic, New York, 1972, pp. 221–260.